polymerase and X genes. HBV replicates its genome via reverse transcription of pregenome RNA. Reverse transcription conducted by viral polymerase takes place after encapsidation of pregenome RNA, resulting in minus-strand DNA synthesis. The RNA template is simultaneously degraded by RNaseH activity, and single-stranded (SS) HBV DNA is constructed. Subsequently, viral polymerase mediates production of plus-strand DNA from minus-strand DNA. In this process, appropriate template switches for primer translocation and circularization lead to the formation of relaxed circular (RC) HBV DNA, whereas the extension *in situ* without template switches results in the formation of duplex linear (DL) HBV DNA [9–11]. The virion containing RC viral DNA has been shown to be more infectious than those containing DL viral DNA in duck hepatitis B virus (DHBV) [12].

In this study, we examined an elderly patient with chronic HBV infection showing fatal exacerbation accompanied by an increase in the viral replicative level. The viruses obtained before and after exacerbation were longitudinally studied. The virus before exacerbation lacked competence for RC HBV DNA synthesis and virion secretion, but the virus after exacerbation had recovered it. Resurgent RC HBV DNA synthesis and virion secretion as the prime causes of disease deterioration originated in conversion of the preS/S gene from a hypermutated to a hypomutated state. This is a novel type of the HBV genomic variation associated with the development of HBV-related fulminant liver disease.

2. Materials and methods

2.1. Case presentation

The patient described in this study was a 83-year-old Japanese male with type B chronic hepatitis. At the initial phase, he was free of symptoms. His alanine aminotransferase (ALT) fluctuated over a range of 50–160 IU/l. Hepatitis B surface antigen (HBsAg) was weakly positive (2^5 according to reversed passive hemagglutination assay), and HBV DNA was below the detection limit based on the slot-blot hybridization assay on day 29. However, after 1 year, he suddenly became fatigued and anorexic. ALT rose to 729 IU/l accompanied by an increase of HBsAg titer (>2^{12}) and the detectable level of HBV DNA on day 374. He was hospitalized due to diagnosis of acute exacerbation of chronic HBV infection. After hospitalization, ALT declined to 150–250 IU/l, but HBV DNA continued to be detectable. The total bilirubin reached up to 5.0 mg/dl on day 418 and increased thereafter. On day 508, he died of hepatic failure despite intensive treatment. Liver histology at autopsy showed features of massive liver necrosis superimposed on chronic non-cirrhotic liver disease. During follow-up, he tested negative for both hepatitis B e antigen (HBeAg) and antibody to HBeAg by radioimmunoassay. Antibody to HBsAg was also negative according to passive hemagglutination assay. The clinical course of the patient is summarized in Fig. 1. Informed consent was obtained from his family members. Serum samples collected on day 29 (1 year before exacerbation, designated as P1) and day 407 (after exacerbation, designated as P2) were stored at −80 °C and used for this study. HBV DNA levels as measured by the PCR-based assay (Amplicor HB Monitor, Roche Diagnostics) using stored sera at P1 and P2 were $10^{5.4}$ and $10^{8.6}$ copies/ml.

2.2. PCR, sequencing and subcloning

To obtain the full-length HBV DNA strains before and after exacerbation, PCR reaction was carried out using stored sera at P1 and P2. After DNA extraction, the DNA was amplified for 35 cycles using Taq/Pwo DNA polymerase (Roche Diagnostics) according to the method described by Günther et al. [13]. The primers were BF1 (5′-CCGGAAAGCTTGAGCTCTTCTTTTTCACCTCTGCCTAATCA-3′, nt 1821–1841) and BR1 (5′-CCGGAAAGCTTGAGCTCTTCAAAAAG TTGCATGGTGCTGG-3′, nt 1825–1806), both of which had a SapI recognition site at the 5′ end. After brief incubation with Taq polymerase to create A overhang, the PCR product was cloned into the plasmid pCR-TOPO4 (Invitrogen). To avoid misreading in the PCR reaction, nucleotide sequences of six independent full-length HBV DNA clones were determined. Nucleotides that were detected in only one clone at the corresponding nucleotide position were excluded. If necessary, the interchange in the portion of HBV DNA using plural number of clones, or site-directed mutagenesis,

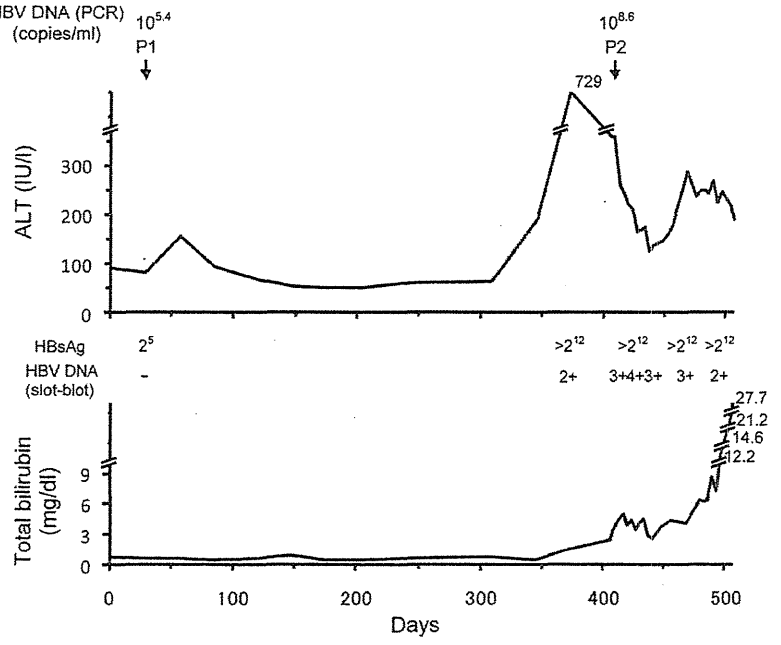

Fig. 1. Clinical course of a patient with type B chronic hepatitis showing fatal exacerbation.

was conducted. Finally, the HBV strains, FEP1 and FEP2 (GenBank Accession Nos. AB485809 and AB485810), were obtained as predominant viruses at P1 and P2. These two HBV strains were subjected to phylogenetic tree analysis along with representative HBV strains of various genotypes.

2.3. Plasmid constructs

Plasmid pHBC had 1.2 times the genomic length of HBV DNA and expressed the wild-type genotype C HBV strain adr4 (GenBank Accession No. X01587) [14]. As for the HBV strains FEP1 and FEP2, the full-length HBV DNA fragment was removed from the pCR-TOPO4 by SapI digestion, followed by synthesis of circular double-stranded HBV DNA by T4 ligase treatment. Based on this, the HBV-expressing plasmids pFEP1 and pFEP2, which carried the 1.2-fold HBV genome, were constructed. pFEch1 and pFEch2, made by swapping the BstEII/BstBI fragment between pFEP1 and pFEP2, expressed the chimeric HBV strains FEch1 and FEch2. For trans-complementation analysis, another plasmid pHBV1.5, which expressed wild-type genotype A HBV strain adw2 (GenBank Accession No. X02763) [15], was used. pHBV1.5Δpol and pHBV1.5ΔS lacked production of the polymerase protein and all surface proteins, respectively, due to insertion of the in-frame stop codon. pCMV-SEAP expressed a secreted alkaline phosphatase.

2.4. Examination for mixed viral population

To examine the mixed viral population in the preS/S gene, PCR-subcloning analysis was performed. The DNA fragment encompassing the whole preS2/S gene was amplified by PCR using the primers BF5 (5′-AAGAGACAGTCATCCTCAGG-3′ nt 3183–3202) and BR7 (5′-GGGTTCAAATGTATACCCAA-3′, nt 839–820). The PCR

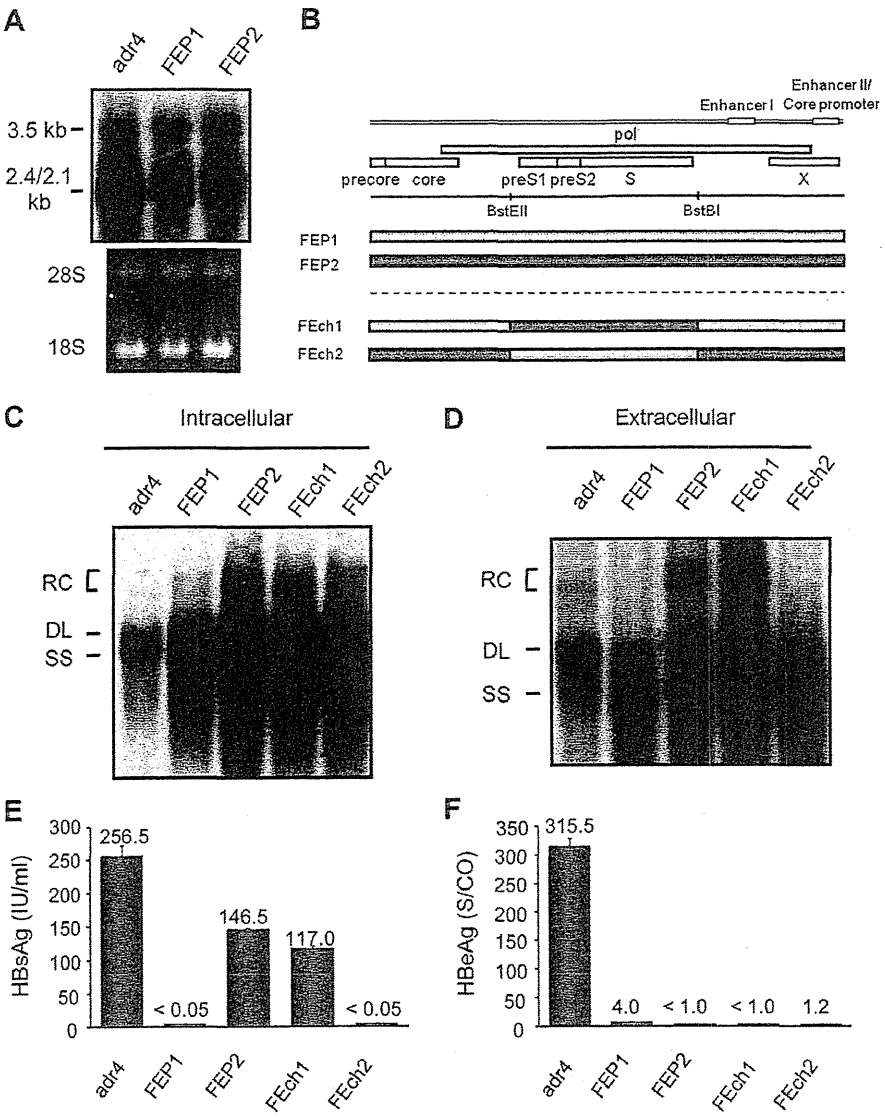

Fig. 2. Viral transcription, replication, virion secretion and antigen production of FEP1 and FEP2, and their chimeric constructs in transfected cells. (A) HBV transcripts in transfected cells examined by Northern blot analysis. The lower panel indicates ethidium bromide staining as a loading control. (B) A scheme of chimeric HBV strains, FEch1 and FEch2. (C) Intracellular progeny HBV DNA in transfected cells examined by Southern blot analysis. (D) Extracellular progeny HBV DNA in transfected cells examined by Southern blot analysis. (E) Secreted HBsAg in the culture supernatant of transfected cells. Data were expressed as IU/ml. (F) Secreted HBeAg in the culture supernatant of transfected cells. Data were expressed as the ratio of optical density of the sample to the cut-off value (S/CO). SS, single-stranded HBV DNA; DL, duplex linear HBV DNA; RC, relaxed circular HBV DNA.

product was cloned into the plasmid pCR-TOPO4, and inserted HBV DNA sequences of independent clones were determined. As another examination of the mixed viral population, PCR was done to obtain the short HBV DNA fragment including the preS2 deletion site using the primers BF-11 (5′-AAGAGACAGTCATCCTCAGG-3′, nt 3183–3202) and BR-11 (5′-AACTGGAGCCACCAGCAGGA-3′, nt 74–55). Next, the product was electrophoresed on polyacrylamide gel. In this assay, the various ratios of the mixture of plasmids pFEP1 and pFEP2 were used as templates of the PCR reaction. Consequently, a minor population of the virus could be detected if it was present at approximately one-tenth of the total population.

2.5. Transfection study

Huh7 cells (7×10^5 cells) were seeded on a 60-mm-diameter culture dish and transfected with 2 μg of various HBV-expressing plasmids and 0.1 μg of pCMV-SEAP using the FuGENE6 reagent (Roche Diagnostics). In transcomplementation analysis, 1 μg of pFEP1 was cotransfected with 1 μg of pHBV1.5Δpol, pHBV1.5ΔS or pBluescriptIISK$^+$ (mock). The cellular nucleic acid and culture supernatant were collected on day 5 after transfection. The alkaline phosphatase activity in the culture supernatant was measured to evaluate transfection efficiency.

For Northern blot analysis to detect HBV transcripts, the total RNA was extracted using an TRIzol reagent (Invitrogen), followed by RNase-free DNaseI treatment, phenol/chloroform extraction and ethanol precipitation. The sample was then electrophoresed in a formaldehyde–agarose denaturing gel, transferred onto a nylon membrane, hybridized with alkaline phosphatase-labeled HBV DNA probe and detected with the chemiluminescent substrate CDP-star (GE Healthcare Life Sciences). Southern blot analyses to detect intracellular and extracellular progeny HBV DNAs were carried out as described elsewhere [16]. Secreted HBsAg and HBeAg in the culture supernatant were measured by chemiluminescent immunoassay. All transfection experiments were done at least three times, and the representative results are shown.

3. Results

3.1. Differences in viral sequences between FEP1 and FEP2 strains were most prominent in the preS/S gene

The HBV strains FEP1 and FEP2, obtained before and after fatal exacerbation of the patient with chronic HBV infection, were classified as genotype C2, the most prevalent genotype in Japan, according to the phylogenetic tree analysis (data not shown). FEP1 and FEP2 had sequence divergences of 3.1% and 2.8% from the representative wild-type genotype C2 HBV strain adr4 [14] and differed by 0.8% from each other. Amino acid substitutions in the preS/S, precore/core, X and polymerase gene in adr4, FEP1 and FEP2 strains are shown in the Supplementary Tables 1 and 2. FEP1 had 20 amino acid substitutions in the preS/S gene, 6 in the precore/core gene, 5 in the X gene and 34 in the polymerase gene, whereas FEP2 had 10 in the preS/S gene, 7 in the precore/core gene, 5 in the X gene and 30 in the polymerase gene compared with adr4. As for comparison between FEP1 and FEP2, substitutions were noted at 15 amino acid residues in the preS/S gene, one in the precore/core gene, none in the X gene and 14 in the polymerase gene. In addition, FEP1, but not FEP2, had a 12-bp deletion in the preS2 gene, a 9-bp deletion in the S gene, and the in-frame stop codon in the distal S gene, which caused truncation of preS/S and polymerase proteins. As for other peculiarities of the FEP1 and FEP2 strains, both had the A1896, T1762/A1764 and C1753 mutations, which have been shown to be frequently detected in fulminant hepatitis [2–4], and disruption of the start codon of the preS2 gene, which has been reported to be commonly found in chronic HBV infection [17]. Thus, FEP1 and FEP2 strains differed considerably in nucleotide sequences from the wild-type adr4 strain. Further-

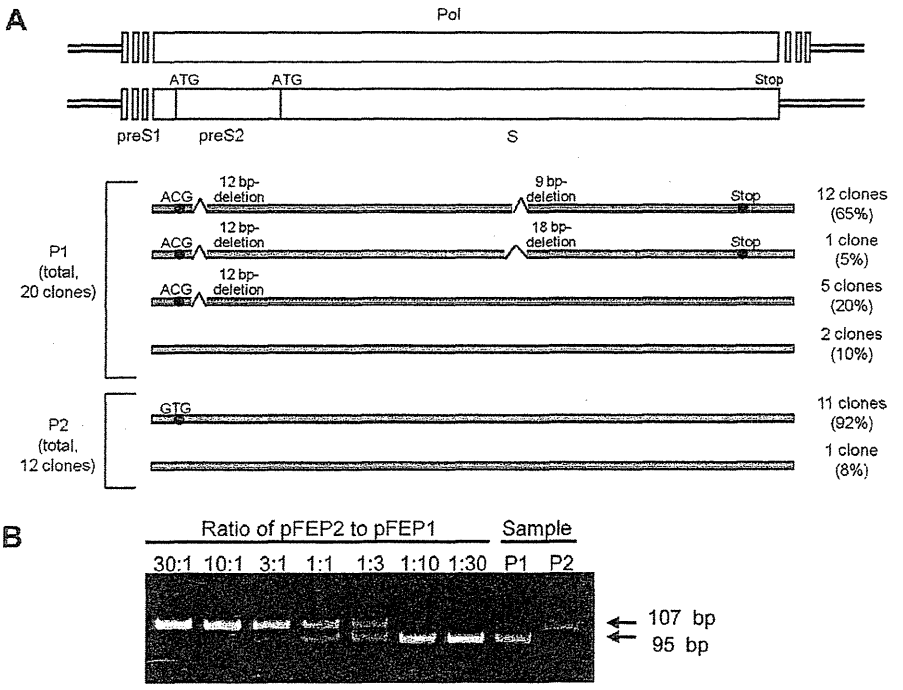

Fig. 3. Mixed viral population in the preS/S gene in a patient with type B chronic hepatitis showing fatal exacerbation. (A) A scheme of the result of PCR-subcloning analysis. The HBV fragment encompassing the whole preS2/S gene was amplified by PCR and subcloned. Next, the independent clones were used for sequencing analysis. A total of 20 and 12 independent clones derived from serum samples P1 and P2 were examined. (B) A representative result of PCR amplification of short HBV DNA fragment including the preS2 deletion site. The product derived from HBV DNA without the deletion was 109 bp long, whereas that derived from HBV DNA with the deletion was 95 bp long.

more, the differences between FEP1 and FEP2 in the sequences were the most prominent in the preS/S gene.

3.2. FEP1 lacked competence for RC HBV DNA synthesis and RC HBV DNA-containing virion secretion but FEP2 possessed it

Next, we investigated viral transcription, DNA synthesis, virion secretion and antigen production in the wild-type adr4 strain, and the patient-derived FEP1 and FEP2 strains using *in vitro* transfection analysis. The levels of HBV transcripts did not differ among the three strains (Fig. 2A). When the levels of intracellular and extracellular progeny HBV DNAs were compared (Fig. 2C and D), both FEP1 and FEP2 revealed more synthetic activity of HBV DNA than adr4 in the intracellular HBV DNA assay, but the differences in the levels of extracellular HBV DNA among adr4, FEP1 and FEP2 were modest. According to these findings, FEP1 and FEP2 strains may possess increased activity of viral encapsidation and/or minus-strand DNA synthesis compared with adr4, whereas wild-type adr4 strain may be superior to FEP1 and FEP2 in the efficient virion secretion. When the differences between FEP1 and FEP2 were examined with respect to the intracellular and extracellular HBV DNA assays, RC HBV DNA synthesis and RC HBV DNA-containing virion secretion were seriously impaired in FEP1, compared with FEP2 (Fig. 2C and D). Regarding the levels of secreted HBsAg and HBeAg, HBsAg was not detected in FEP1 but detectable in adr4 and FEP2 (Fig. 2E). Both FEP1 and FEP2 could not synthesize HBeAg (Fig. 2F), because they harbored the precore-defective A1896 mutation.

3.3. Inability of RC HBV DNA synthesis and of RC HBV DNA-containing virion secretion in FEP1 were responsible for the preS/S gene

The most remarkable difference in the viral genome between FEP1 and FEP2 was observed in the preS/S gene. Therefore, chimeric HBV strains, FEch1 and FEch2, constructed by swapping the entire preS/S region between FEP1 and FEP2 (Fig. 2B), were examined. As shown in Fig. 2C and D, RC HBV DNA synthesis and RC HBV DNA-containing virion secretion were seen in FEch1 but had been prevented in FEch2. Also, HBsAg was detected in FEch1 but not in FEch2 (Fig. 2E). Both FEch1 and FEch2 did not produce HBeAg (Fig. 2F). Thus, incompetence of RC HBV DNA synthesis and of virion secretion in FEP1 were responsible for the preS/S gene.

3.4. Wild-type-like HBV strain coexisted with FEP1 strain

We further examined the detailed viral population at P1 and P2. PCR-subcloning assay was done for the preS2/S gene, which showed the regions with the most differences in sequences between FEP1 and FEP2 (Fig. 3A). Thirteen of 20 clones derived from P1 had the two short deletions in the preS2 and S genes, the in-frame stop codon in the distal S gene and disruption of the preS2 start codon, as was the case for FEP1 strain. Five clones possessed only the deletion in the preS2 gene and disruption of the preS2 start codon. The remaining two clones had none of these mutations and deletions and were similar to the wild-type strain. As for clones derived from P2, 11 of the 12 clones showed disruption of the preS2 start codon, whereas the remaining one clone did not. In PCR analysis for the short region containing the preS2 deletion site (Fig. 3B), the virus with preS2 deletion was predominant, but approximately one-tenth of the virus without deletion was also detected at P1. Only the virus without the deletion was seen at P2. According to these observations, the wild-type-like HBV strain with minimal viral genomic variations in the preS/S gene coexisted as a minor population at P1.

3.5. RC HBV DNA synthesis and virion secretion were transcomplemented by the preS/S protein

Finally, we investigated whether the wild-type-like virus coexisting as a minor population can complement the inability of RC HBV DNA synthesis and virion secretion in FEP1 strain *in trans*. As shown in Fig. 4A, transfection with pHBV1.5 yielded synthesis of RC, DL and SS HBV DNAs, whereas transfection with pHBV1.5ΔS resulted in less amounts of RC HBV DNA than that with pHBV1.5. Transfection with pHBV1.5Δpol showed complete absence of HBV DNA synthesis. As for transcomplementation analysis (Fig. 4B and C), cotransfection of pHBV1.5Δpol with pFEP1 did not augment RC HBV DNA synthesis in the intracellular HBV DNA assay, but led to enhanced secretion of RC HBV DNA-containing virion in the extracellular HBV DNA assay. By contrast, cotransfec-

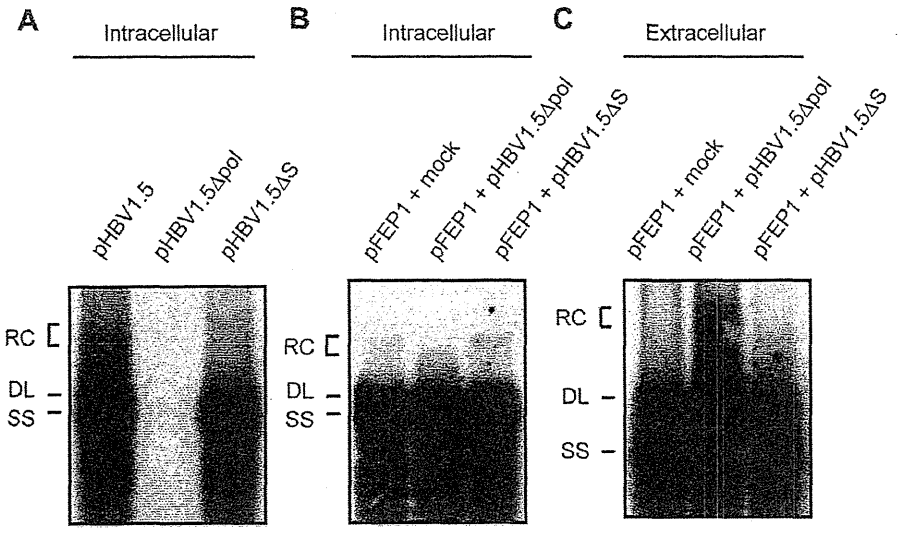

Fig. 4. Transcomplementation of insufficient viral secretion in FEP1 strain by HBV-expressing constructs, pHBV1.5Δpol and pHBV1.5ΔS. (A) Intracellular progeny HBV DNA in cells transfected with pHBV1.5, pHBV1.5Δpol and pHBV1.5ΔS by Southern blot analysis. (B) Intracellular progeny HBV DNA in cells cotransfected of pFEP1 with mock, pHBV1.5Δpol and pHBV1.5ΔS by Southern blot analysis. (C) Extracellular progeny HBV DNA in cells cotransfected of pFEP1 with mock, pHBV1.5Δpol and pHBV1.5ΔS by Southern blot analysis. SS, single-stranded HBV DNA; DL, duplex linear HBV DNA; RC, relaxed circular HBV DNA.

tion of pHBV1.5ΔS with pFEP1 could not compensate for the inability of RC HBV DNA synthesis and virion secretion. These results suggest that insufficiency of RC HBV DNA synthesis and virion secretion in FEP1 may be transcomplemented not by the polymerase protein but by the preS/S protein of the wild-type-like HBV strain.

4. Discussion

The present study describes a patient with type B chronic hepatitis who showed fatal exacerbation accompanied by more than 10^3-fold increment of viral replicative activity. The predominant HBV strains FEP1 and FEP2, obtained before and after exacerbation, were investigated to clarify what viral genomic alterations triggered disease deterioration. FEP1 and FEP2 possessed considerably different nucleotide sequences including A1896, T1762/A1764 and C1753 mutations, that have been reported to be frequently detected in the fulminant hepatitis-related HBV strain, compared with the wild-type strain [2–4]. Not only FEP2 and but also FEP1 revealed more overall synthetic activity of HBV DNA than the wild-type strain. Thus, both FEP1 and FEP2 were potent highly-replicative strains. As for the most significant difference between FEP1 and FEP2, FEP1 lacked competence for RC HBV DNA synthesis and RC HBV DNA-containing virion secretion, whereas FEP2 maintained it. Because of the difference in the virological feature between them, FEP1 was not very pathogenic, but FEP2 became a highly virulent strain. These results indicate that resurgent RC HBV DNA synthesis and virion secretion may lead to the onset of fulminant liver disease in this patient.

Chimeric analysis revealed that the preS/S gene, where FEP1 had a considerable number of mutations and deletions but FEP2 did not, accounted for the difference in the ability of RC HBV DNA synthesis and virion secretion between FEP1 and FEP2. In addition, insufficient RC HBV DNA synthesis and virion secretion in FEP1 were transcomplemented not by the polymerase protein but by the preS/S protein of the wild-type virus. Although mutations and deletions in the preS/S gene observed in FEP1 certainly affect the properties of both preS/S and polymerase proteins, disability of the preS/S protein rather than the polymerase protein may be responsible for the inability of RC HBV DNA synthesis and virion secretion in FEP1. By contrast, FEP2 may produce the competent preS/S protein to accomplish RC HBV DNA synthesis and virion secretion because of fewer mutations in the preS/S gene. Taken together, conversion from a hypermutated to a hypomutated state in the preS/S gene may have been the strain-specific viral genomic change serving as the primitive cause of lethal disease deterioration in our patient.

Examination for viral population showed that the wild-type-like strain carrying no mutations in the preS/S gene coexisted as a minor population with the predominant strain epitomized by FEP1 before exacerbation. Transcomplementation analysis also revealed that the wild-type-like HBV strain may function as a helper virus that compensates for impaired synthesis of RC HBV DNA and virion secretion in FEP1 strain. This may be a reason why the patient already had a certain degree of viral replication and chronic liver inflammation before exacerbation.

A few investigators reported secretion-defective HBV strains with the mutations in the S gene derived from patients with fulminant hepatitis and those with chronic HBV infection [8,18]. Regarding the former strain, the secretion-defective strain was isolated after the onset of fulminant hepatitis, suggesting the pathogenic importance of the deficiency in the viral antigen secretion itself [8]. This does not agree with our findings because the virus lacking the ability of RC HBV DNA-containing virion secretion was not very pathogenic, but the virus having it triggered fulminant liver disease in our study. Further work should be done to clarify the involvement of the secretion-defective HBV in various clinical manifestations.

In the process of plus-strand DNA synthesis, the presence or absence of template switches for primer translocation and circularization determines the preference for RC HBV DNA synthesis. Appropriate template switches and subsequent RC HBV DNA synthesis require donor and acceptor sites for template switches and several other *cis*-acting sequences [10,11]. FEP1 is, to our knowledge, the first naturally-occurring HBV strain displaying incompetence of RC HBV DNA synthesis and virion secretion. Such incompetence in FEP1 was compensated not by the polymerase protein but by the preS/S protein of the wild-type HBV. This lets us hypothesize that the preS/S protein may play a pivotal role in the secretion of RC HBV DNA-containing virus and possibly, the synthesis of RC HBV DNA. The preS/S protein, as well as the polymerase protein and *cis*-acting sequences within the viral genome, may be an important component for efficient RC HBV DNA formation. The hypothesis is also supported by our other finding that the synthetic activity of RC HBV DNA was lower in cells transfected with pHBV1.5ΔS than in those transfected with pHBV1.5.

In summary, we identified a novel type of the viral genomic variation associated with the development of fulminant liver disease in the longitudinal virological study of a type B chronic hepatitis patient showing fatal exacerbation. The virus before exacerbation revealed insufficiency of RC HBV DNA synthesis and virion secretion, but the virus after exacerbation had the ability for both. The change in the virological character was based on conversion from a hypermutated to a hypomutated status in the preS/S gene, which may be the main cause for disease deterioration in the patient. Our findings offer a new insight into the pathogenesis of HBV-related fulminant liver disease.

Appendix A. Supplementary data

Supplementary data associated with this article can be found, in the online version, at doi:10.1016/j.bbrc.2010.02.114.

References

[1] W.M. Lee, Acute liver failure, N. Engl. J. Med. 329 (1993) 1862–1872.
[2] M. Omata, T. Ehata, O. Yokosuka, K. Hosoda, M. Ohto, Mutations in the precore region of hepatitis B virus DNA in patients with fulminant and severe hepatitis, N. Engl. J. Med. 324 (1991) 1699–1704.
[3] S. Sato, K. Suzuki, Y. Akahane, K. Akamatsu, K. Akiyama, K. Yunomura, F. Tsuda, T. Tanaka, H. Okamoto, Y. Miyakawa, M. Mayumi, Hepatitis B virus strains with mutations in the core promoter in patients with fulminant hepatitis, Ann. Intern. Med. 122 (1995) 241–248.
[4] T. Imamura, O. Yokosuka, T. Kurihara, T. Kanda, K. Fukai, F. Imazeki, H. Saisho, Distribution of hepatitis B viral genotypes and mutations in the core promoter and precore regions in acute forms of liver disease in patients from Chiba, Japan. Gut 52 (2003) 1630–1637.
[5] T.F. Baumert, S.A. Rogers, K. Hasegawa, T.J. Liang, Two core promoter mutations identified in a hepatitis B virus strain associated with fulminant hepatitis result in enhanced viral replication, J. Clin. Invest. 98 (1996) 2268–2276.
[6] T.F. Baumert, C. Yang, P. Schürmann, J. Köck, C. Ziegler, C. Grüllich, M. Nassal, T.J. Liang, H.E. Blum, F. von Weizsäcker, Hepatitis B virus mutations associated with fulminant hepatitis induce apoptosis in primary Tupaia hepatocytes, Hepatology 41 (2005) 247–256.
[7] I. Pult, T. Chouard, S. Wieland, R. Klemenz, M. Yaniv, H.E. Blum, A hepatitis B virus mutant with a new hepatocyte nuclear factor 1 binding site emerging in transplant-transmitted fulminant hepatitis B, Hepatology 25 (1997) 1507–1515.
[8] T. Kalinina, A. Riu, L. Fischer, H. Will, M. Sterneck, A dominant hepatitis B virus population defective in virus secretion because of several S-gene mutations from a patient with fulminant hepatitis, Hepatology 34 (2001) 385–394.
[9] D. Ganem, A.M. Prince, Hepatitis B virus infection, natural history and clinical consequences, N. Engl. J. Med. 350 (2004) 1118–1129.
[10] N. Liu, L. Ji, M.L. Maguire, D.D. Loeb, Cis-Acting sequences that contribute to the synthesis of relaxed-circular DNA of human hepatitis B virus, J. Virol. 78 (2004) 642–649.
[11] E.B. Lewellyn, D.D. Loeb, Base pairing between cis-acting sequences contributes to template switching during plus-strand DNA synthesis in human hepatitis B virus, J. Virol. 81 (2007) 6207–6215.

[12] W. Yang, J. Summers, Infection of ducklings with virus particles containing linear double-stranded duck hepatitis B virus DNA: Illegitimate replication and reversion, J. Virol. 72 (1998) 8710–8717.
[13] S. Günther, B.C. Li, S. Miska, D.H. Kruger, H. Meisel, H. Will, A novel method for efficient amplification of whole hepatitis B virus genomes permits rapid functional analysis and reveals deletion mutants in immunosuppressed patients, J. Virol. 69 (1995) 5437–5444.
[14] A. Fujiyama, A. Miyanohara, C. Nozaki, T. Yoneyama, N. Ohtomo, K. Matsubara, Cloning and structural analyses of hepatitis B virus DNAs, subtype adr, Nucleic Acids Res. 11 (1983) 4601–4610.
[15] V. Bruss, D. Ganem, The role of envelope proteins in hepatitis B virus assembly, Proc. Natl. Acad. Sci. USA 88 (1991) 1059–1063.
[16] K. Ohkawa, T. Takehara, M. Kato, M. Deguchi, M. Kagita, H. Hikita, A. Sasakawa, K. Kohga, A. Uemura, R. Sakamori, S. Yamaguchi, T. Miyagi, H. Ishida, T. Tatsumi, N. Hayashi, Supportive role played by precore and preS2 genomic changes in the establishment of lamivudine-resistant hepatitis B virus, J. Infect. Dis. 198 (2008) 1150–1158.
[17] G. Raimondo, L. Costantino, G. Caccamo, T. Pollicino, G. Squadrito, I. Cacciola, S. Brancatelli, Non-sequencing molecular approaches to identify preS2-defective hepatitis B virus variants proved to be associated with severe liver diseases, J. Hepatol. 40 (2004) 515–519.
[18] N. Khan, M. Guarnieri, S.H. Ahn, J. Li, Y. Zhou, G. Bang, K.H. Kim, J.R. Wands, S. Tong, Modulation of hepatitis B virus secretion by naturally occurring mutations in the S gene, J. Virol. 78 (2004) 3262–3270.

Biochemical and Biophysical Research Communications 394 (2010) 574–580

Contents lists available at ScienceDirect

Biochemical and Biophysical Research Communications

journal homepage: www.elsevier.com/locate/ybbrc

Alterations in hepatitis B virus nucleotide sequences in a chronic virus carrier from immunotolerant to immunoactive phase

Kazuyoshi Ohkawa [a,b], Tetsuo Takehara [a], Tomohide Tatsumi [a], Hisashi Ishida [a], Matsuo Deguchi [c], Masanori Kagita [c], Atsushi Hosui [a], Takuya Miyagi [a], Kazuhiro Katayama [b], Norio Hayashi [a,*]

[a] Department of Gastroenterology and Hepatology, Osaka University Graduate School of Medicine, 2-2, Yamadaoka, Suita 565-0871, Japan
[b] Department of Hepatobiliary and Pancreatic Oncology, Osaka Medical Center for Cancer and Cardiovascular Diseases, 1-3-3, Nakamichi, Higashinari-ku, Osaka 537-8511, Japan
[c] The Laboratory for Clinical Investigation, Osaka University Hospital, 2-15, Yamadaoka, Suita 565-0871, Japan

ARTICLE INFO

Article history:
Received 21 February 2010
Available online 7 March 2010

Keywords:
Chronic hepatitis B virus infection
Immunotolerant phase
Immunoactive phase
Viral replicative competence
Virus-specific immune response

ABSTRACT

Factors involved in transition from the immunotolerant to immunoactive phase in chronic hepatitis B virus (HBV) infection remain unclear. We investigated viral mutations occurring during transition and elucidated their virological and immunological significance. Full-length HBV DNA sequences were serially determined in a chronic HBV carrier from the immunotolerant to immunoactive phase. Viral replicative competence was examined by transfection analysis. HBV-specific $CD8^+$ T cell response was evaluated by coculture of $CD8^+$ T cells with autologous dendritic cells followed by interferon-γ Elispot assay. Eleven point mutations and two deletions appeared around the onset of the immunoactive phase. Viral replicative competence declined significantly after the onset of active hepatitis. Examination of the $CD8^+$ T cell response against two putative T-cell epitopes, which contained substituted amino acids from the immunotolerant to immunoactive phase, showed that mutant HBV epitopes gave a lesser T cell response than wild-type HBV ones. In summary, point mutations and deletions may occur prior to or concurrent with the onset of the immunoactive phase during chronic HBV infection. These mutations may result in a significant decrease in both viral replicative competence and HBV-specific $CD8^+$ T cell response, suggesting a possible adaptation for the maintenance of viral persistence.

1. Introduction

More than 350 million people worldwide suffer from chronic hepatitis B virus (HBV) infection [1]. A chronic HBV carrier state is mainly established by virus infection during the perinatal period or childhood because of the immature immune system. The majority of chronic HBV carriers is thought to be responsible for mother-to-child transmission of the virus, especially in Asian countries.

In the natural course of chronic HBV infection, the initial phase is an immunotolerant one, which is characterized by positive hepatitis B e antigen (HBeAg), high HBV DNA, normal alanine aminotransferase (ALT), and no or minimal histological inflammation. It usually persists for 10–40 years in perinatally infected patients, followed by an immunoactive phase. This phase is based on the occurrence of immune system-mediated cytotoxicity toward HBV-infected hepatocytes, leading to ALT elevation and active liver inflammation. A high HBV DNA level and positive HBeAg still continue. The long-festering immunoactive phase frequently results in the development of cirrhosis and hepatocellular carcinoma. On the other hand, loss of HBeAg or seroconversion to antibody to HBeAg (anti-HBe) is associated with the reduction of HBV DNA and alleviation of liver inflammation [2].

HBV is noncytopathic in itself, and its disease pathogenesis is largely mediated by the cellular immune response. In particular, the $CD8^+$ cytotoxic T lymphocyte (CTL) is thought to play an important role in both viral clearance and liver cell injury [3]. It has been reported that a strong HBV-specific CTL response was detected in individuals with type B acute self-limited hepatitis but not in those with chronic HBV infection [4,5]. The crucial role of $CD8^+$ T cells in the pathogenesis of HBV-related liver disease has recently been confirmed in the HBV-infected chimpanzee system [6].

What remains unclear are the factors associated with the transition from the immunotolerant to immunoactive phase in chronic HBV infection. HBV mutations are speculated to be one of the factors related to the onset of active liver injury. Several cross-sectional studies have shown that chronic HBV carriers in the immunoactive phase tended to possess more mutations in the core promoter/enhancer II region and core gene than those in the immunotolerant phase [7–9]. However, to better understand the possible link of HBV mutations with the shift from the immunotolerant to immunoactive phase, detailed longitudinal evaluation of HBV mutations should be done for an individual patient.

* Corresponding author.
E-mail address: hayashin@gh.med.osaka-u.ac.jp (N. Hayashi).

0006-291X/$ - see front matter © 2010 Elsevier Inc. All rights reserved.
doi:10.1016/j.bbrc.2010.03.022

This issue led us to examine a chronic HBV carrier who was initially in the immunotolerant phase and changed over to the immunoactive phase after 8.3 years of follow-up. Alterations in the full-length HBV DNA sequences were examined using serial serum samples collected around the transition period of both phases. We further investigated the influences of mutations occurring from the immunotolerant to immunoactive phase on the viral replicative competence and virus-specific $CD8^+$ T cell response.

2. Methods

2.1. Patient clinical course and sampling points

The patient examined in the present study was a 30-year-old female (Fig. 1). She first visited Osaka University Hospital in January 1998, because she had been pointed out as having tested positive for hepatitis B surface antigen (HBsAg) at another hospital. From the beginning, she was diagnosed as being in the immunotolerant phase of chronic HBV infection as recognized by positive HBeAg, high HBV DNA of >1000 Meq/ml by the branched DNA assay (Chiron) and low ALT of <20 IU/l. Antibody to HBsAg (anti-HBs) and anti-HBe were negative. She was followed-up at 3- to 6-month intervals. The immunotolerant phase of chronic HBV infection continued for 8.3 years until April 2006. In October 2006, ALT rose slightly to 31 IU/l, although it was below the upper limit of the normal range (≤40 IU/l). In February 2007, she developed active hepatitis accompanied by an increase in ALT to an abnormal level. The ALT fluctuated thereafter and increased up to 489 IU/l in March 2008. HBV DNA as detected by the PCR-based assay (Amplicor HB Monitor, Roche), measured since June 2004, was maintained at a high level of ≥8.5 log copies/ml even after the onset of active hepatitis, but slightly decreased to 7.7 log copies/ml in March 2008. Subsequently, she received entecavir treatment (0.5 mg/day), resulting in the sustained HBV DNA clearance (<2.6 log copies/ml) and ALT normalization, although the HBeAg remained positive in May 2009, the end of follow-up.

From June 2004 to January 2008, a total of eight serial serum samples were stored at −80 °C and used for sequencing analysis. The sampling points were designated as P1–P8; P1, June 2004 (ALT, 17 IU/l); P2, December 2005, (ALT, 20 IU/l); P3, April 2006 (ALT, 20 IU/l); P4, October 2006 (ALT, 31 IU/l); P5, February 2007 (ALT, 70 IU/l); P6, March 2007 (ALT, 110 IU/l); P7, July 2007 (ALT, 143 IU/l); and P8, January 2008 (ALT, 279 IU/l). According to changes in ALT, the patient was in the immunotolerant phase at P1–P3 and entered the immunoactive phase at P5–P8. The period around P4 was considered to be the transitional phase. The heparinized blood sample was also collected in May 2009, 14 months of entecavir treatment (P9; ALT 10 IU/l) for the immunological analysis concerning the $CD8^+$ T cell response against the HBV-derived epitopes. Informed consent was obtained from the patient.

2.2. HBV markers

HBsAg, anti-HBs, HBeAg, and anti-HBe were measured by enzyme immunoassay or chemiluminescent immunoassay. HBV DNA was detected by the Amplicor HB Monitor (Roche). The 100-fold diluted serum sample was used, if necessary.

2.3. PCR-direct sequencing for determining nucleotide sequences of full-length HBV DNA

PCR-direct sequencing was conducted for full-length HBV DNA, whose experimental method is shown in Supplementary material 1. The nucleotide sequences of full-length HBV DNA derived from

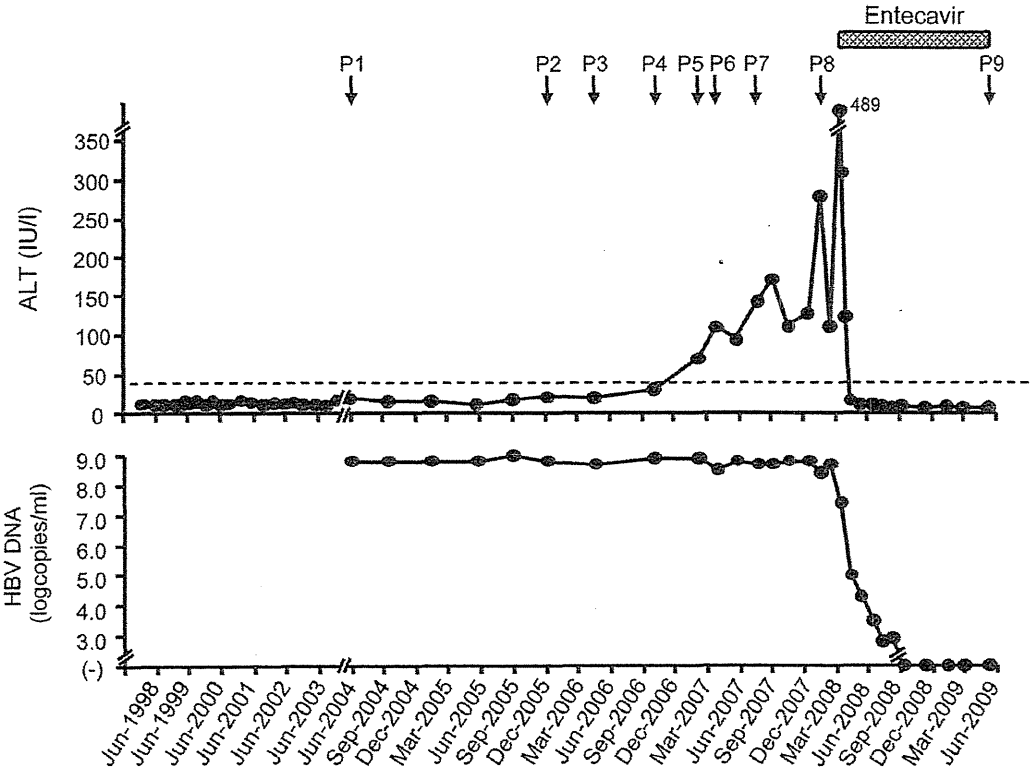

Fig. 1. Clinical course and sampling points of a patient with chronic HBV infection who was followed-up from immunotolerant to immunoactive phase. Arrows indicate the sampling points P1 to P9.

the serum sample at P1 (designated as HBV-IT strain) are shown in the International DNA database (Accession No. AB485808).

2.4. Amplification of full-length HBV DNA and identification of deletion mutant HBV

The PCR amplification of full-length HBV DNA was done according to the method described by Günther et al. [10]. The primers were BF1 (5′-CCG GAA AGC TTG AGC TCT TCT TTT TCA CCT CTG CCT AAT CA-3′, nt 1821–1841) and BR1 (5′-CCG GAA AGC TTG AGC TCT TCA AAA AGT TGC ATG GTG CTG G-3′, nt 1825–1806), both of which had a SapI recognition site at their 5′ end. The smaller-than-expected PCR product corresponding to the deletion mutant HBV DNA was cloned into the plasmid pCR-TOPO4 (Invitrogen), and several clones were picked up for sequencing analysis.

2.5. Transfection of circular double-stranded HBV DNA synthesized from the PCR product

In this study, the full-length HBV DNA amplified by PCR was subjected to the transfection analysis. Briefly, the serum sample containing the 6.5 log copies of HBV DNA was used for the PCR amplification using the BF1/BR1 primer set. The PCR product (50 μl) was purified with a spin column and digested with 10 U of SapI at 37 °C for 16 h. After purification using a spin column again, the sample was circularized by brief incubation with T4 ligase. Finally, Huh-7 cells (3×10^6 cells) were seeded onto the 60-mm diameter culture dish and transfected with the circular double-stranded full-length HBV DNA synthesized from the PCR product using the Fugene 6 reagent (Roche).

2.6. Detection of progeny HBV DNA and secreted HBV antigen in transfected cells

On day 3 after transfection, the cellular lysate and culture medium were collected to examine the progeny HBV DNA and secreted HBsAg and HBeAg. The progeny HBV DNA was detected by Southern blot analysis as described elsewhere [11]. HBsAg and HBeAg in the culture media were examined by chemiluminescent immunoassay.

2.7. Prediction of HBV-derived peptide epitopes

The genotyping assay for HLA-A and -B alleles from the whole blood-derived DNA by the PCR-sequencing-based typing method (SRL) revealed that the patient expressed HLA-A*2402/*3303 and -B*4403/*5201. The entire amino acid sequences of the preS/S, precore/core, polymerase, and X proteins of the HBV-IT strain were reviewed for 9- and 10-mer peptides that could possess binding activity to HLA class I molecules using a peptide-motif scoring system supplied online by National Institutes of Health (http://bimas.dcrt.nih.gov/molbio/hla_bind). The analysis was carried out for HLA-A*2402, -A*3302 (instead of -A*3303), -B*4403, and -B*5201. The HBV-derived peptides containing the substituted sites in amino acid sequences from the immunotolerant to immunoactive phase were screened. Two 9-mer "wild-type" peptides derived from the HBV-IT strain, SDYCLTHLV ($Pol_{335-343}$) and LGEEIRLKV ($X_{123-131}$), which had high scores for the binding affinity to HLA-B*5201 molecules, were selected for immunological analysis. Two additional "mutant" peptides, SDYCLTHIV and LGEEIRLMI, where substituted amino acid residues occurring from the immunotolerant to immunoactive phase are underlined, were also examined in comparison with the wild-type peptides. All peptides had been synthesized by Sigma–Aldrich with >90% purity.

2.8. Culture and stimulation of peripheral blood lymphocytes

Peripheral blood mononuclear cells were isolated from the heparinized blood sample by Ficoll-Hypaque density gradient centrifugation and cultured at 37 °C for 1 h. Non-adherent "T cell-enriched" cells were stored at −80 °C. The adherent cells were further cultured with 10 ng/ml of recombinant human granulocyte macrophage colony-stimulating factor (PeproTech) and 10 ng/ml of recombinant human interleukin-4 (PeproTech) for 1 week to generate dendritic cells (DCs). Autologous $CD8^+$ T cells were isolated from the non-adherent cells using the specific magnetic beads (MACS, Miltenyi Biotec). DCs (2×10^5 cells) were cocultured with 2×10^6 of $CD8^+$ T cells in the presence of 10 μg/ml of HBV-derived peptides for 1 week. Finally, the responder $CD8^+$ T cells were subjected to the interferon-γ Elispot assay.

2.9. Detection of HBV-derived peptide-reactive $CD8^+$ T cells by interferon-γ Elispot assay

To assess the frequencies of peripheral blood $CD8^+$ T cells recognizing the particular HBV epitopes, the interferon-γ Elispot assay was carried out as previously described [12]. The experimental method is shown in Supplementary material 2.

2.10. Statistical analysis

Student's non-paired *t* test and the one-way analysis of variance were used as appropriate. *p* Values less than 0.05 were considered to be statistically significant.

3. Results

From the serum sample at P1, the full-length HBV DNA sequence was determined by PCR-direct sequencing analysis and designated as the HBV-IT strain. This strain had no apparent mixed viral populations at all nucleotide positions as far as this sequencing analysis could detect. The HBV-IT strain was classified as genotype C2, the most prevalent HBV genotype in Japan, as examined by phylogenetic tree analysis (data not shown). All point mutations occurring from the immunotolerant to immunoactive phase are presented in Fig. 2. From P1 to P8, there were a total of 11 point mutations, A125 (causing pol-L342I), C441 (causing surface-V96A), A1613 (causing pol-R841K), G1614 (causing x-T81A), T1762 (causing x-K130M), A1764 (causing x-V131I), C1938 (causing core-V13A), T2088 (causing core-G63V), C2137 (silent), T2357 (causing core-G153C and pol-E17D), and T2444 (causing the in-frame stop codon). The T2444 mutation resulted in truncation of the core protein by two amino acids. All mutations began to emerge at P3–P5 as a minor viral population and became predominant thereafter, although the mixed viral population with and without the point mutations was still observed at P8.

Next, we carried out PCR amplification of the full-length HBV DNA to assess the existence of deletion mutant HBV using serum samples at P1, P4, P6, and P8. As shown in Fig. 3A, there were no deletion mutant HBV strains at P1. However, a small amount of deleted HBV DNA was detected at P4. At P6 and P8, the deletion mutant HBV accumulated, whereas the full-length HBV declined gradually. PCR-subcloning analysis revealed the existence of two kinds of deletion mutant HBVs (Fig. 3B). One had a deletion 1257 bp long, and the other had two deletions 282 bp and 1269 bp long. In both types of mutant HBV strains, deletions were involved in the core, polymerase and preS/S genes.

The patient possessed a homogeneous viral population in the initial immunotolerant phase, but the virus existed as a mixture of wild-type and various types of mutant viral strains around the

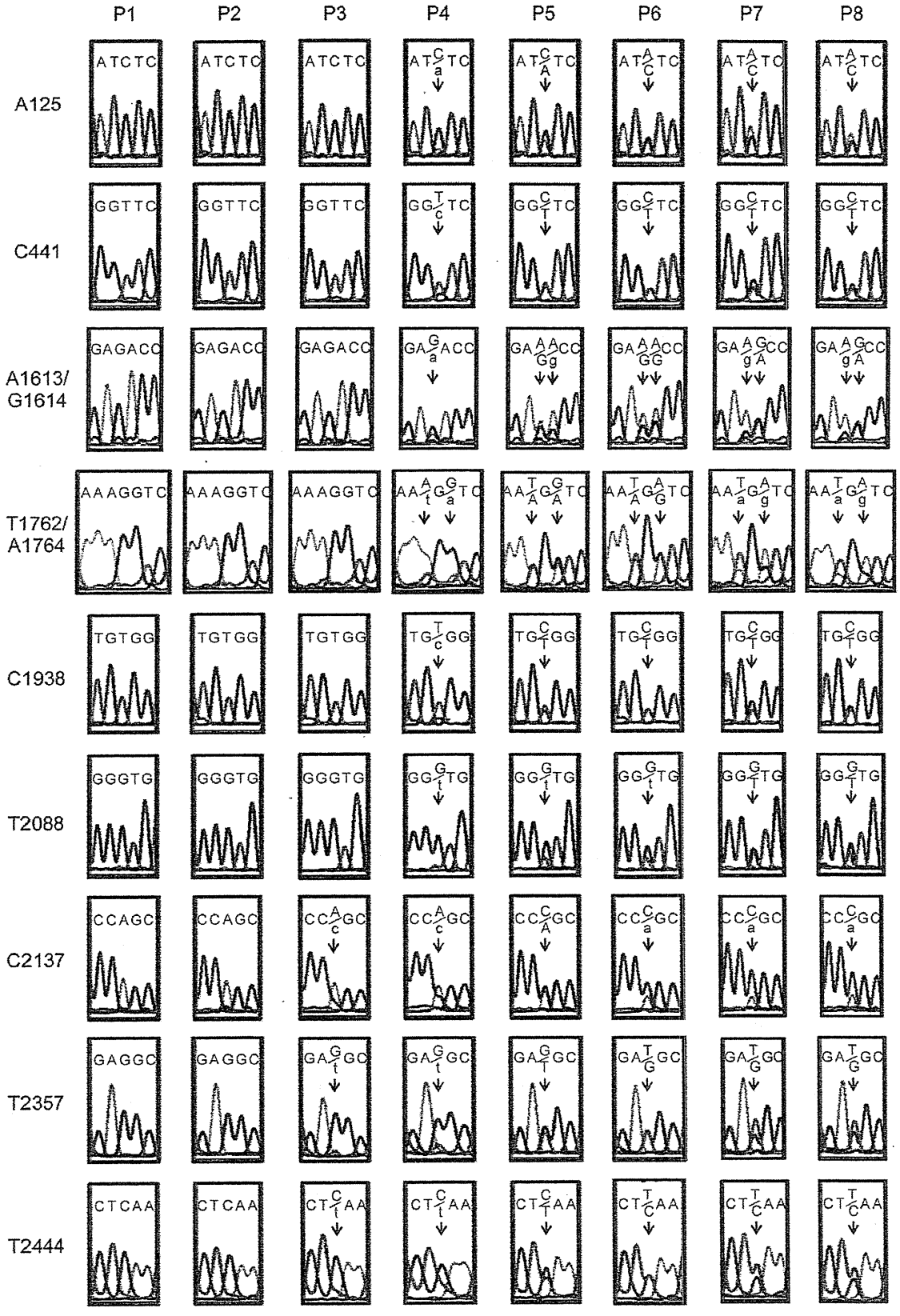

Fig. 2. Point mutations occurring in a patient with chronic HBV infection from immunotolerant to immunoactive phase. The full-length HBV nucleotide sequences were determined by PCR-direct sequencing analysis using serum samples obtained at P1 to P8. Point mutations appearing from P1 to P8 are indicated by arrows.

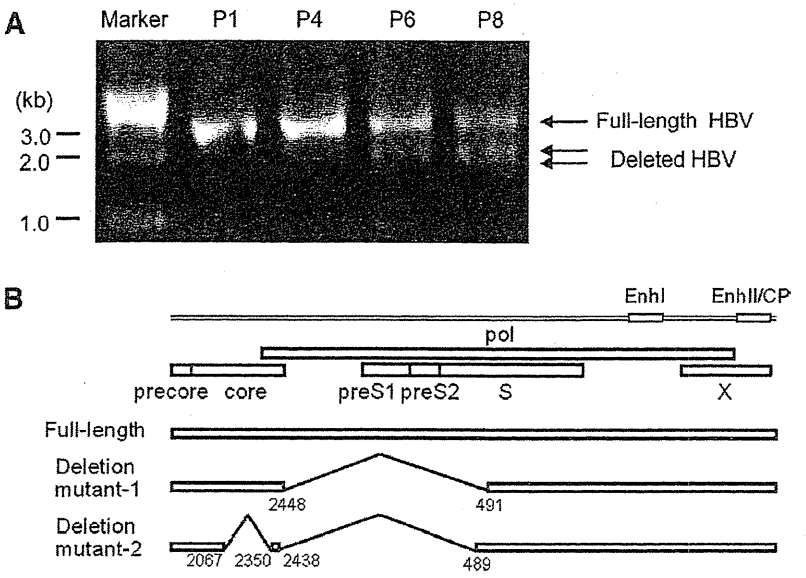

Fig. 3. Detection and identification of deletion mutant HBV DNA in a patient with chronic HBV infection from the immunotolerant to immunoactive phase. (A) Detection of full-length and deletion mutant HBV DNAs by PCR assay. (B) A schematic diagram of the deletion mutant HBV DNAs (-1 and -2) derived from the patient.

onset of immunoactive phase. To overcome the heterogeneity of the viral population and to investigate overall replicative competence of the virus in a single host, we carried out transfection analysis not using HBV-expressing plasmid constructs but using the circular double-stranded HBV DNA synthesized directly from the PCR products at P1, P4, P6, and P8. The progeny HBV DNA after transfection was examined as a marker of viral replicative competence. As shown in Fig. 4A and B, the progeny HBV DNA decreased gradually with time ($p < .005$), and the level was reduced by approximately 4-fold at P8, compared to that at P1. Similarly, the production of HBsAg and HBeAg declined significantly from P1 to P8 ($p < .001$ and $p < .01$) (Supplementary Fig. 1A and B).

Finally, we evaluated the influence of HBV mutations occurring from the immunotolerant to immunoactive phase on the $CD8^+$ T cell response against HBV epitopes. Two HBV-IT strain-derived T-cell epitopes, $Pol_{335-343}$ and $X_{123-131}$, which included the substituted amino acids from the immunotolerant to immunoactive phase, were selected using an algorism to identify the potential binding site to the particular HLA class I molecules. Peripheral blood mononuclear cells were obtained from the patient at the remission phase after entecavir treatment. $CD8^+$ T cells were cocultured with autologous DCs in the presence of "wild-type" or "mutant" HBV-derived peptides. The HBV epitope-specific T cell response was evaluated with the interferon-γ Elispot assay. The frequencies of $CD8^+$ T cells specific for the mutant HBV $Pol_{335-343}$ SDYCLTHIV peptide were lower than those for the wild-type SDYCLTHLV peptide (Fig. 4C). Also, the frequencies of $CD8^+$ cells specific to the mutant HBV $X_{123-131}$ LGEEIRLMI peptide were lower than those to the wild-type LGEEIRLKV peptide (Fig. 4D). Thus, with respect to these two HBV epitopes, the mutations detected around the onset of active liver inflammation led to a decrease in the HBV-specific $CD8^+$ T cell response.

4. Discussion

The precise mechanisms, through which the immune-mediated active liver inflammation breaks out following an asymptomatic immunotolerant phase, have not been elucidated in chronic HBV infection. To shed new light on this, we investigated the involvement of HBV mutations in the transition from the immunotolerant to immunoactive phase. A chronic HBV carrier undergoing the long-term follow-up was examined in this study, and the full-length HBV sequences were serially determined. A total of 11 point mutations were observed from the immunotolerant to immunoactive phase. Most of these mutations were detected prior to or concurrent with transition of both phases. In addition, emergence of the deletion mutation coincided with the onset of the immunoactive phase. Thus, point mutations and deletions were found to be generated closely associated with the shift to the immunoactive phase in chronic HBV infection. Regarding the virus population in the patient, the homogeneous viral population without point mutations and deletions was observed in the initial immunotolerant phase. Around the same time as the onset of active hepatitis, the virus with point mutations and deletions began to appear as a minor viral population and became predominant with time accompanied by worsening of liver inflammation.

The 11 point mutations observed during the follow-up of the patient led to a total of 10 amino acid substitutions of various HBV proteins and one in-frame stop codon formation in the distal core gene. Two of the 11 mutations were the well-known T1762/A1764 in the basic core promoter, which has been frequently found in patients with HBV infection in association with low HBeAg production [13]. Furthermore, there were two kinds of deletion mutant virus having a broad range of the deletion sites involving the core, polymerase and preS/S genes.

Viral replicative competence, as examined by in vitro transfection analysis using the synthesized circular double-stranded HBV DNA, declined significantly after the onset of active liver inflammation. This may be mainly due to a relative decrease of the full-length HBV in contrast to an increase of the deletion mutant virus in the immunoactive phase. The mutant HBV with the long deletion, which has been reported to be detected in patients with chronic HBV infection [14], is replication-incompetent, and its replication may be transcomplemented by replication-competent full-length HBV. Such a "defective" deletion mutant virus may have an inhibitory effect on replication of the wild-type virus, as has been suggested in the case of HBV with the core internal deletion mutation [15]. In addition, some of the point mutations may directly reduce viral replicative activity, although the effect of each point mutation on viral replication remained to be verified in this study.

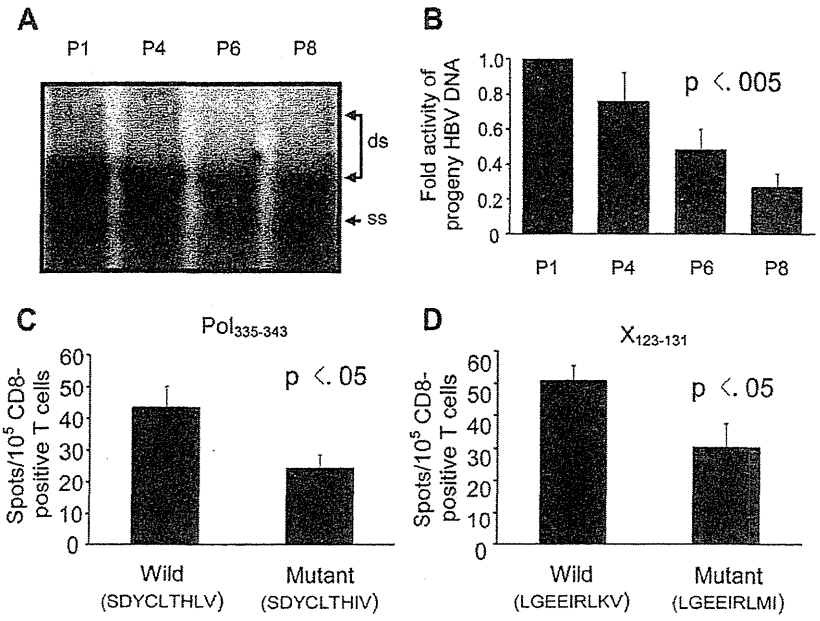

Fig. 4. (A,B) Levels of progeny HBV DNA in Huh-7 cells transfected with circular double-stranded HBV DNA synthesized from the PCR product. (A) A representative result of Southern blot analysis for detection of progeny HBV DNA in transfected cells. ss, single-stranded HBV DNA. ds, double-stranded HBV DNA. (B) Quantitative analysis of the level of progeny HBV DNA examined by Southern blot analysis and image analyzing procedure. The level of progeny HBV DNA in the case of transfection with the circular double-stranded HBV DNA derived from the sample at P1 was considered as 1, and the fold activities in the case of transfection with those derived from the samples at P4, P6 and P8 were calculated. (C,D) $CD8^+$ T cell responses against $Pol_{335-343}$ (C) and $X_{123-131}$ (D) epitopes in the HBV-IT strain. $CD8^+$ T cells were cocultured with autologous DCs in the presence of wild-type or mutant HBV-derived peptides. HBV epitope-specific T cell response was evaluated by interferon-γ Elispot assay. Interferon-γ spots per 10^5 $CD8^+$ cells were analyzed. All experiments were done three times, and the results are shown as mean ± SD.

They may be reasons for reduced viral replicative competence in the immunoactive phase compared with the immunotolerant phase.

We further investigated the influence of HBV mutations occurring from the immunotolerant to immunoactive phase on the $CD8^+$ T cell response against the particular HBV epitopes. Two putative HLA B^*5201-restricted T-cell epitopes, which contained the substituted amino acid residue from the immunotolerant to the immunoactive phase, were studied. The HBV epitope-specific $CD8^+$ T cell response was evaluated using the interferon-γ Elispot assay. The results showed that the mutant HBV epitopes provided a lesser $CD8^+$ T cell response than the wild-type HBV ones, suggesting that the mutant virus may have less susceptibility to the CTL than the wild-type virus. According to our finding, the HBV mutations emerging before or simultaneously with the onset of the immunoactive phase may lead to less responsiveness to the CTL and insufficient viral clearance.

In our immunological analysis, peripheral blood mononuclear cells were collected after the entecavir treatment-induced remission phase. Previous studies revealed that patients with acute HBV infection display a robust virus-specific CTL response, whereas the response in patients with chronic HBV infection is generally weak [4,5]. It has also been shown that hyporesponsiveness of CTL can be restored in patients with chronic HBV infection after antiviral treatment-induced remission [16]. In this regard, usage of the blood sample after entecavir treatment may have been better than that before treatment for efficient detection of the HBV-specific $CD8^+$ T cell response in our patient. Although the delayed sampling point in our immunological assay may have biased the result of analysis, our finding may offer a piece of suggestive information from a viewpoint of the immunological aspect in chronic HBV infection.

In conclusion, we showed that, in the detailed analysis of a chronic HBV carrier, point mutations and deletions occurred prior to or concurrently with the onset of the immunoactive phase during the course of chronic HBV infection. The virus having point mutations and deletions emerged as a minor viral population and became predominant with time accompanied by worsening of active liver inflammation. In chronic HBV infection, it is speculated that the onset of active liver inflammation following the inactive immunotolerant phase may be due to a restored immune response against antigens of the pre-existing "wild-type" virus, which may be triggered by unknown mechanisms. It is of particular note that the "mutant" virus possessing various point mutations and deletions may reveal a significant decrease in both viral replicative competence and virus-specific $CD8^+$ T cell response compared with the "wild-type" virus. This may be a possible adaptation mechanism for the maintenance of viral persistence in chronic HBV infection.

Appendix A. Supplementary data

Supplementary data associated with this article can be found, in the online version, at doi:10.1016/j.bbrc.2010.03.022.

References

[1] W.M. Lee, Hepatitis B virus infection, N. Engl. J. Med. 337 (1997) 1733–1745.
[2] G. Fattovich, F. Bortolotti, F. Donato, Natural history of chronic hepatitis B: special emphasis on disease progression and prognostic factors, J. Hepatol. 48 (2008) 335–352.
[3] F.V. Chisari, C. Ferrari, Hepatitis B virus immunopathogenesis, Annu. Rev. Immunol. 13 (1995) 29–60.
[4] A. Penna, F.V. Chisari, A. Bertoletti, G. Missale, P. Fowler, T. Giuberti, F. Fiaccadori, C. Ferrari, Cytotoxic T lymphocytes recognize an HLA-A2-restricted epitope within the hepatitis B virus nucleocapsid antigen, J. Exp. Med. 174 (1991) 1565–1570.
[5] R. Nayersina, P. Fowler, S. Guilhot, G. Missale, A. Cerny, H.J. Schlicht, A. Vitiello, R. Chesnut, J.L. Person, A.G. Redeker, F.V. Chisari, HLA A2 restricted cytotoxic T lymphocyte responses to multiple hepatitis B surface antigen epitopes during hepatitis B virus infection, J. Immunol. 150 (1993) 4659–4671.

[6] R. Thimme, S. Wieland, C. Steiger, J. Ghrayeb, K.A. Reimann, R.H. Purcell, F.V. Chisari, CD8(+) T cells mediate viral clearance and disease pathogenesis during acute hepatitis B virus infection, J. Virol. 77 (2003) 68–76.
[7] T. Ehata, M. Omata, O. Yokosuka, K. Hosoda, M. Ohto, Variations in codons 84–101 in the core nucleotide sequence correlate with hepatocellular injury in chronic hepatitis B virus infection, J. Clin. Invest. 89 (1992) 332–338.
[8] K. Takahashi, K. Aoyama, N. Ohno, K. Iwata, Y. Akahane, K. Baba, H. Yoshizawa, S. Mishiro, The precore/core promoter mutant (T1762A1764) of hepatitis B virus: clinical significance and an easy method for detection, J. Gen. Virol. 76 (1995) 3159–3164.
[9] K. Zhang, F. Imazeki, K. Fukai, M. Arai, T. Kanda, R. Mikata, O. Yokosuka, Analysis of the complete hepatitis B virus genome in patients with genotype C chronic hepatitis in relation to HBeAg and anti-HBe, J. Med. Virol. 79 (2007) 683–693.
[10] S. Günther, B.C. Li, S. Miska, D.H. Kruger, H. Meisel, H. Will, A novel method for efficient amplification of whole hepatitis B virus genomes permits rapid functional analysis and reveals deletion mutants in immunosuppressed patients, J. Virol. 69 (1995) 5437–5444.
[11] K. Ohkawa, T. Takehara, M. Kato, M. Deguchi, M. Kagita, H. Hikita, A. Sasakawa, K. Kohga, A. Uemura, R. Sakamori, S. Yamaguchi, T. Miyagi, H. Ishida, T. Tatsumi, N. Hayashi, Supportive role played by precore and preS2 genomic changes in the establishment of lamivudine-resistant hepatitis B virus, J. Infect. Dis. 198 (2008) 1150–1158.
[12] T. Tatsumi, C.J. Herrem, W.C. Olso, J.H. Finke, R.M. Bukowski, M.S. Kinch, E. Ranieri, W.J. Storkus, Disease stage variation in CD4+ and CD8+ T-cell reactivity to the receptor tyrosine kinase EphA2 in patients with renal cell carcinoma, Cancer Res. 63 (2003) 4481–4489.
[13] H. Okamoto, F. Tsuda, Y. Akahane, Y. Sugai, M. Yoshiba, K. Moriyama, T. Tanaka, Y. Miyakawa, M. Mayumi, Hepatitis B virus with mutations in the core promoter for an e antigen-negative phenotype in carriers with antibody to e antigen, J. Virol. 68 (1994) 8102–8110.
[14] F. Schläge, S. Schaefer, M. Metzler, N. Gratzki, F. Lampert, W.H. Gerlich, R. Repp, Quantitative DNA fragment analysis for detecting low amounts of hepatitis B virus deletion mutants in highly viremic carriers, Hepatology 32 (2000) 1096–1105.
[15] T.T. Yuan, M.H. Lin, D.S. Chen, C. Shih, A defective interference-like phenomenon of human hepatitis B virus in chronic carriers, J. Virol. 72 (1998) 578–584.
[16] C. Boni, A. Penna, G.S. Ogg, A. Bertoletti, M. Pilli, C. Cavallo, A. Cavalli, S. Urbani, R. Boehme, R. Panebianco, F. Fiaccadori, C. Ferrari, Lamivudine treatment can overcome cytotoxic T-cell hyporesponsiveness in chronic hepatitis B: new perspectives for immune therapy, Hepatology 33 (2001) 963–971.

Research Article

EASL EUROPEAN ASSOCIATION FOR THE STUDY OF THE LIVER | JOURNAL OF HEPATOLOGY

Altered interferon-α-signaling in natural killer cells from patients with chronic hepatitis C virus infection☆

Takuya Miyagi[1,2], Tetsuo Takehara[1], Kumiko Nishio[1], Satoshi Shimizu[1], Keisuke Kohga[1], Wei Li[1], Tomohide Tatsumi[1], Naoki Hiramatsu[1], Tatsuya Kanto[1], Norio Hayashi[1,2,*]

[1]*Department of Gastroenterology and Hepatology, Osaka University Graduate School of Medicine, Suita, Osaka, Japan;* [2]*Global Centers of Excellence Program, Frontier Biomedical Science Underlying Organelle Network Biology, Osaka University, Suita, Osaka, Japan*

Background & Aims: Natural killer (NK) cells play an important role in the immune response against virus infection. Interferon (IFN)-α, an essential component in therapy against hepatitis C virus (HCV) infection, regulates NK cell function. However, it remains obscure how chronic HCV infection (CHC) modifies intracellular IFN-α signaling in NK cells. We investigated IFN-α signaling in NK cells in patients with CHC.

Methods: Peripheral blood mononuclear cells were obtained from patients with CHC and healthy subjects (HS) as controls.

Results: The expression level of signal transducer and activator of transcription (STAT) 1, a key molecule of IFN-α signaling, was clearly higher in NK cells from the CHC patients than in those from HS. The phosphorylation level of STAT1 with IFN-α stimulation was significantly greater in NK cells from the CHC patients than in those from the HS, while that of STAT4 was significantly less. These phosphorylation levels of STAT1 and STAT4 positively and negatively correlated with the STAT1 level in NK cells, respectively. The IFN-α induced messenger RNA level of the suppressor of cytokine signaling 1, which is a downstream gene of phosphorylated-STAT1, was clearly greater in NK cells from the CHC patients than in those from the HS, while that of IFN-γ, which is a downstream gene of phosphorylated-STAT4, was clearly lower.

Conclusions: These results indicate altered IFN-α signaling in NK cells in CHC patients, suggesting that this alteration is associated with the persistence of HCV infection and resistance to IFN-α therapy.

Keywords: Natural killer cells; Interferon; Hepatitis C virus; Signal transducer and activator of transcription.

Received 28 October 2009; received in revised form 24 March 2010; accepted 28 March 2010; available online 25 May 2010

☆ Funding: The authors who have taken part in this study declared that they do not have anything to disclose regarding funding or conflict of interest with respect to this manuscript.

* Corresponding author. Address: Department of Gastroenterology and Hepatology, Osaka University Graduate School of Medicine, 2-2 Yamada-oka, Suita, Osaka 565-0871, Japan. Tel.: +81 6 6879 3621; fax: +81 6 6879 3629.

E-mail address: hayashin@gh.med.osaka-u.ac.jp (N. Hayashi).

Abbreviations: NK, natural killer; IFN, interferon; STAT, signal transducer and activator of transcription; HCV, hepatitis C virus; CHC, chronic hepatitis C virus infection; HS, healthy subject; SOCS, suppressor of cytokine signaling; mRNA, messenger RNA; PBMC, peripheral blood mononuclear cell; IL, interleukin; pSTAT, phosphorylated-signal transducer and activator of transcription; RT-PCR, reverse transcription polymerase chain reaction; NKT, natural killer T; ISG, interferon stimulated gene.

Introduction

Natural killer (NK) cells play an important role in innate immune responses against a variety of viral infections by directly killing infected cells with cytotoxic molecules such as perforin and granzyme [1]. The cells also have a great ability to secrete a key cytokine, interferon (IFN)-γ, which activates subsequent adaptive immune responses as well as inhibits viral replication [1,2]. Another major component in innate immune responses during viral infections is IFN-α, which is the most abundant cytokine released during viral infections [3]. In addition to its anti-viral effects, IFN-α activates NK cells to induce IFN-γ production via activation of the signal transducer and activator of transcription (STAT) 4, as well as its cytotoxic ability via activation of STAT1 [4–7].

Hepatitis C virus (HCV) causes persistent infection in more than 70% of infected patients. Whereas some of the patients show a carrier-like state, most develop chronic liver diseases, including chronic hepatitis, liver cirrhosis, and hepatocellular carcinoma, which is why HCV infection is a worldwide health problem [8]. The administration of IFN-α is a well-established anti-viral therapy for HCV infection. More than 90% of patients with acute HCV infection respond to IFN-α based therapy, while only around 50% of patients with chronic HCV infection (CHC) do [9–12], suggesting a mechanism by which persistent HCV infection leads to resistance to IFN-α based therapy. NK cell number has been demonstrated to decrease in patients with CHC, while it is controversial whether NK cell functions are impaired in patients with CHC [13–15]. It thus remains unclear whether perturbation of NK cells is involved in the persistence of CHC as well as resistance to the therapy [13–15].

In the present study, we investigated how chronic HCV infection modifies intracellular IFN-α signaling in NK cells. The expression level of total STAT1, a key molecule of IFN-α signaling, was clearly higher in NK cells from patients with CHC than in those from healthy subjects (HS). Phosphorylation of STAT1, resulting in induction of the suppressor of cytokine signaling (SOCS) 1 messenger RNA (mRNA) expression in response to IFN-α was clearly greater in NK cells from the CHC patients than

in those from the HS. On the other hand, the phosphorylation of STAT4, resulting in induction of IFN-γ mRNA expression in response to IFN-α, was clearly less in NK cells from the CHC patients than in those from the HS. NK cell degranulation was significantly enhanced in response to IFN-α in the HS, but not in the CHC patients. These findings suggest altered IFN-α signaling in NK cells in patients with CHC. The alteration of IFN-α signaling might be associated with the persistence of chronic HCV infection and resistance to IFN-α therapy.

Materials and methods

Subjects

Twenty-six patients with CHC (HCV RNA genotype 1) and 26 healthy volunteers were enrolled in this study. The profile of these subjects is shown in the Supplementary data and Supplementary Table 1. The study was approved by the ethical committee of Osaka University Hospital.

Isolation of peripheral blood mononuclear cell (PBMC) populations

PBMCs were isolated from fresh heparinized peripheral blood by Ficoll-Hypaque density gradient centrifugation as described [16].

In vitro stimulation of cells

Prepared cells were unstimulated or stimulated with either natural human IFN-α, recombinant human IFN-γ or recombinant human interleukin (IL)-12. The details are provided in the Supplementary data.

Cell lysates and Western blot analysis

Prepared cells were lysed as described [17]. A 25 μg sample of protein was separated on 10% SDS polyacrylamide gels and transferred onto PVDF membrane. Monoclonal anti-STAT1 antibody (1/Stat1) was purchased from BD Biosciences (San Jose, CA, USA). Polyclonal anti-β-actin antibody from Abcam (Cambridge, MA, USA) was used as the loading control. Detection of immunolabeled proteins was performed as described [17].

Flow cytometric analysis

The staining of prepared cells was performed as described [16,18]. Briefly, cells were stained with fluorescein isothiocyanate-conjugated anti-CD3 (UCHT1) and biotin-conjugated anti-CD56 antibody (B159), fixed and permeabilized with Cytofix/Cytoperm (BD Biosciences) and cold pure methanol, and then stained with phycoerythrin-conjugated anti-phosphorylated-STAT (pSTAT) 4 (pY693) (38/p-Stat4) and Alexa Fluor® 647-conjugated anti-pSTAT1 (pY701) antibody (4a), or phycoerythrin-conjugated anti-STAT1 (1/Stat1) antibody alone, or the corresponding isotype control, followed by staining with peridinin chlorophyll protein-conjugated streptavidin (BD Biosciences). All antibodies were purchased from BD Biosciences. The stained cells were analyzed with a FACScan (Becton Dickinson, Mountain View, CA, USA), and the data were processed using the FlowJo program (Tree Star Inc., Ashland, OR, USA).

NK cell enrichment from PBMCs

To obtain pure populations of $CD56^+$ $CD3^-$ NK cells from PBMCs, NK cells were negatively isolated by magnetic cell sorting with a human NK cell isolation kit (Miltenyi Biotec, Gladbach, Germany). The purity of the isolated population was confirmed using FACS analysis and was more than 90%.

RNA isolation and analysis

Total RNA isolation and the real-time reverse transcription polymerase chain reaction (RT-PCR) analysis are presented in detail in the Supplementary data, Supplementary Fig. 1, and Supplementary Table 2.

NK cell degranulation assay

NK cell degranulation was assessed as described [19], with minor modifications. Details and representative data are provided in the Supplementary data and Supplementary Fig. 2.

Statistical analysis

The statistical significance of differences between the patient and control groups or that of changes due to IFN-α stimulation in the NK cell degranulation assay was determined by applying unpaired or paired Student's *t*-test, respectively. Correlations were assessed using the Pearson product–moment correlation coefficient. The statistical significance was defined as $p < 0.05$.

Results

NK cells from CHC patients showed a higher level of STAT1 expression than those from HS

Murine NK cells have been reported to exhibit a lower level of STAT1 expression than non-NK cells [17,18]. Also, the increase of STAT1 expression level in murine NK cells has been observed in viral infection [18]. We examined whether similar findings could be observed for human NK cells. Western blot analyses revealed that human NK cells from representative HS have a clearly lower level of STAT1 expression than non-NK cells (Fig. 1A). We then examined whether chronic HCV infection affected the STAT1 expression level in NK cells. It was clearly higher in NK cells from the CHC patients than in those from the HS (Fig. 1B).

We next examined STAT1 expression level within individual cells by flow cytometry. Consistent with the results of Western blot analyses, flow cytometric analyses demonstrated that NK cells from a representative healthy subject had a lower level of STAT1 expression than non-NK cells such as T cells or natural killer T (NKT) cells (Fig. 2A). NK cells from a representative CHC patient displayed a clearly higher level of STAT1 expression than

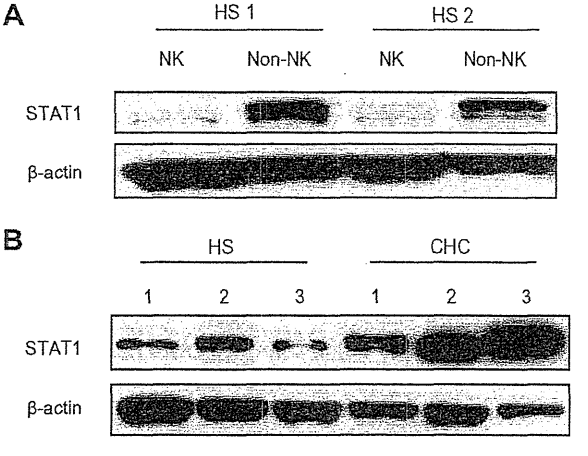

Fig. 1. STAT1 expression in NK cells from patients with chronic HCV infection. STAT1 protein levels were evaluated by Western blot analyses with β-actin measurement as a loading control. PBMCs were obtained from patients with chronic HCV infection (CHC) and healthy subjects (HS). NK cells and non-NK cells were purified from those cells. (A) STAT1 protein levels in NK cells and non-NK cells from two representative HS are shown. (B) STAT1 protein levels in NK cells from three other representative HS and three representative patients are shown.

Research Article

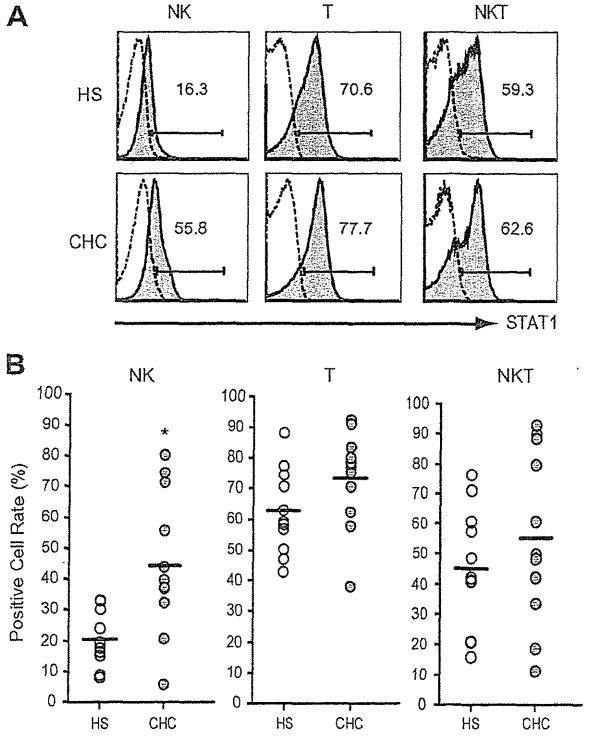

Fig. 2. STAT1 expression level in NK, T or NKT cells from patients with chronic HCV infection. STAT1 protein level was evaluated by flow cytometry, electronically gating on $CD56^+$ $CD3^-$ NK cells, $CD56^-$ $CD3^+$ T cells, and $CD56^+$ $CD3^+$ NKT cells. PBMCs were derived from patients with chronic HCV infection (CHC) and healthy subjects (HS). (A) Representative histograms from a patient and an HS are shown. Dotted lines show staining with the isotype control. Solid lines with shaded areas show staining with the antibody. Numbers are percentages of positive cells (positive cell rate) determined based on the isotype control staining. (B) Comparison of STAT1 expression level between the patients with CHC ($n = 11$) and HS ($n = 11$) are shown as positive cell rates. Each circle represents data for an individual. Horizontal bars represent means. *$p < 0.005$ vs. HS.

those from the healthy subject. Fig. 2B summarizes the profile of the intracellular STAT1 expression level of NK, T, and NKT cells. The intracellular STAT1 expression level of NK cells from the CHC patients was significantly higher than that from the HS, while that of T cells or NKT cells did not show any significant difference.

Altered activation of STAT1/4 occurred in response to IFN-α in NK cells from CHC patients

Activation of STAT1/4 in response to IFN-α in murine NK cells has been reported to shift from pSTAT4 dominant to pSTAT1 dominant as the intracellular STAT1 expression level increases [18]. This led us to examine the activation of STAT1/4 in response to IFN-α in human NK cells using samples from CHC patients and HS. Although IFN-α can phosphorylate both STAT1 and STAT4, IFN-γ can phosphorylate STAT1 and IL-12 can phosphorylate STAT4 in NK cells [1,7]. We examined the phosphorylation level of STAT1/4 in response to IFN-α, compared with IFN-γ or IL-12, in NK cells from the subjects by flow cytometry. It was found that IFN-α phosphorylated STAT1 more strongly in NK cells from the representative CHC patient than in those from the representative HS, while IFN-γ did not (Fig. 3A). On the other hand, IFN-α phosphorylated STAT4 more weakly in NK cells from the CHC patient than in those from the HS, while IL-12 did not. Fig. 3B summarizes the profile of STAT1/4 phosphorylation level in NK cells in response to IFN-α, IFN-γ or IL-12. IFN-α, but not IFN-γ, phosphorylated STAT1 significantly more strongly in NK cells from the CHC patients than in those from the HS. IFN-α, but not IL-12, phosphorylated STAT4 significantly more weakly in NK cells from the CHC patients than in those from the HS. These results suggested altered signaling of IFN-α, but not of IFN-γ or of IL-12, in NK cells of patients with CHC.

We then examined the relationship between STAT1 expression level and STAT1/4 phosphorylation level in response to IFN-α in NK cells from the CHC patients. The phosphorylation level of STAT1 in response to IFN-α correlated significantly and positively with the STAT1 expression level in NK cells ($R^2 = 0.67$, $p < 0.003$), while that of STAT4 correlated significantly and negatively ($R^2 = 0.49$, $p < 0.02$) (Fig. 4). These results suggested that, as in murine NK cells, the activation of STAT1/4 in response to IFN-α in human NK cells shifts from a preference for pSTAT4 to one for pSTAT1 as intracellular STAT1 expression level increases.

Altered induction of interferon stimulated gene (ISG) expression occurred in response to IFN-α in NK cells

We examined how the altered activation of STAT1/4 in response to IFN-α in NK cells affected the induction of downstream gene expression. Real-time RT-PCR analyses revealed that the induction level of SOCS1 mRNA expression with IFN-α stimulation, which is a downstream gene of pSTAT1, was clearly greater in NK cells isolated from the CHC patients than in those from the HS, and that the induction level of IFN-γ mRNA expression with IFN-α stimulation, which is a downstream gene of pSTAT4, was clearly lower (Fig. 5). On the other hand, the mRNA induction level of perforin or granzyme B, which is a cytotoxic molecule induced by IFN-α via pSTAT1, was not greater but modestly lower, suggesting negative regulation by the large induction of SOCS1, which is a negative regulator of the pSTAT1 pathway [20].

Altered activation of NK cells occurred in response to IFN-α

To examine how the altered IFN-α signaling in NK cells affected the activation of NK cells in response to IFN-α, we evaluated the NK cell degranulation ability in response to IFN-α. NK cell degranulation assay showed that CD107a expression, as a marker of degranulation, in the presence of K562 cells was significantly up-regulated in response to IFN-α in NK cells from HS, but not in those from CHC patients (Fig. 6), suggesting altered NK cell activation in response to IFN-α in CHC patients.

Discussion

Both IFN-α and IFN-γ have been observed in sera from patients with CHC [21,22]. Their production may be induced by a host response to HCV within the liver, which would make these IFNs detectable in the systemic circulation of patients with CHC. The present study has shown that NK cells from patients with CHC display higher levels of STAT1 expression compared to those from HS (Fig. 1B and Fig. 2). STAT1 itself is one of the ISGs, whose

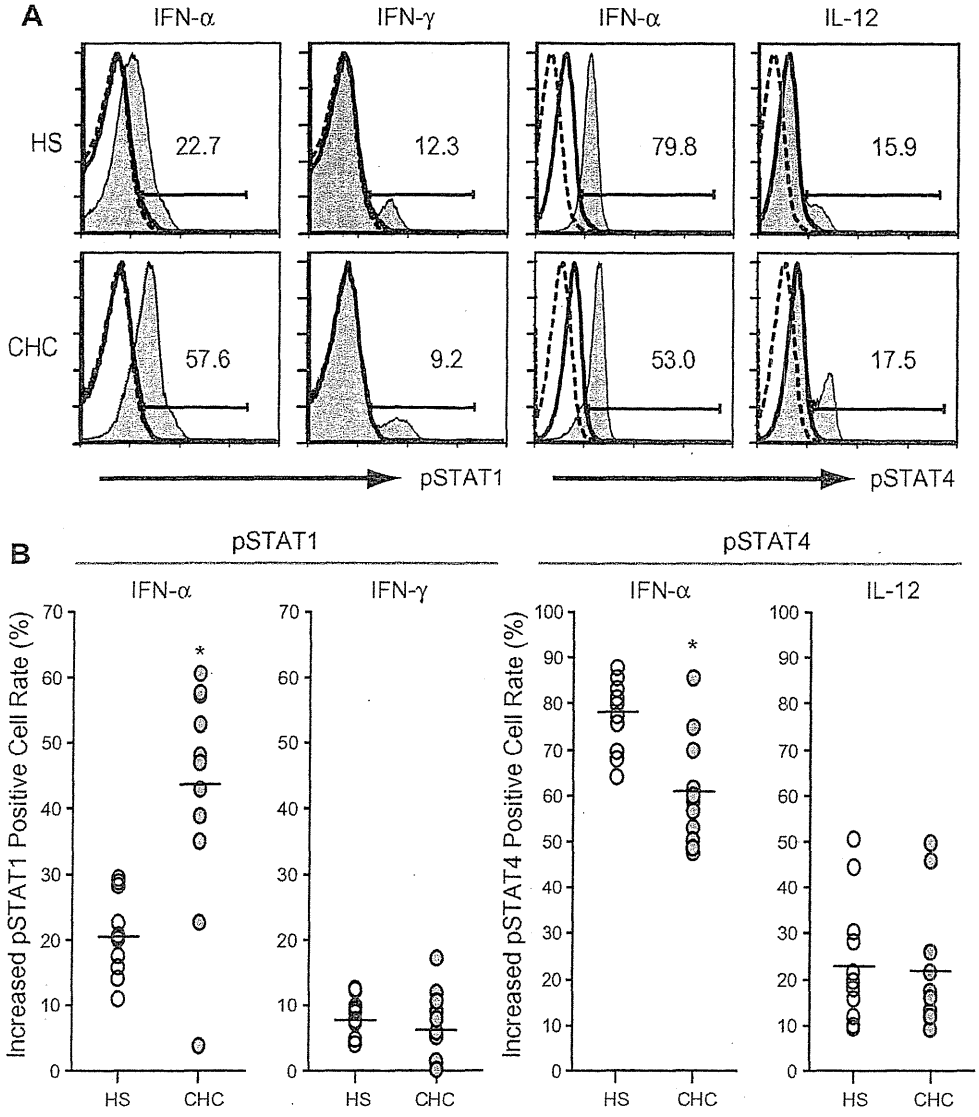

Fig. 3. Altered activation of STAT1/4 in response to IFN-α, but not to IFN-γ or IL-12 in NK cells from patients with chronic HCV infection. pSTAT1 and pSTAT4 protein levels were evaluated by flow cytometry with isotype control staining. PBMCs were derived from patients with chronic HCV infection (CHC) and healthy subjects (HS). (A) Prepared PBMCs were unstimulated or stimulated with natural IFN-α, IFN-γ or IL-12 for 90 min *in vitro*, and then collected. pSTAT1 and pSTAT4 protein levels were evaluated by flow cytometry, electronically gating on $CD56^+$ $CD3^-$ NK cells. Representative histograms of a patient and an HS are shown. Dotted lines show staining of stimulated cells with isotype control. Thick lines show staining of unstimulated cells with the antibody. Thin lines with shaded areas show staining of stimulated cells with the antibody. Positive cell rates were determined based on the staining with isotype controls. Numbers are increased positive cell rates which were determined by subtracting the positive cell rate of unstimulated cells from those of stimulated cells. (B) Comparison of pSTAT1/4 level in response to IFN-α, IFN-γ or IL-12 between the patients with CHC ($n = 11$) and the HS ($n = 11$) are shown as increased pSTAT1/4 positive cell rate. Each circle represents individual data. Horizontal bars represent means. *$p < 0.001$ vs. HS.

expression is up-regulated by IFN-α or IFN-γ [23,24]. It is thus possible that the higher level of STAT1 in NK cells from the CHC patients was up-regulated by IFN-α and/or IFN-γ induced by a chronic host response to HCV.

Our real-time RT-PCR analyses showed that the induction level of SOCS1 mRNA in response to IFN-α was significantly greater in NK cells from the CHC patients than in those from the HS (Fig. 5). This finding is consistent with the observation that the phosphorylation level of STAT1 in response to IFN-α was significantly stronger in NK cells from the CHC patients than in those from the HS (Fig. 3), because SOCS1 is a downstream gene of pSTAT1 [20]. On the other hand, SOCS1 is an inducible negative regulator which inhibits further activation of the pSTAT1 pathway [20]. It is therefore possible that this greater up-regulation of SOCS1 owing to the greater level of STAT1 phosphorylation in response to IFN-α finally results in a weaker response to IFN-α, that is, a weaker induction of ISGs via the pSTAT1 pathway. Indeed, an increase of the STAT1 level,

Research Article

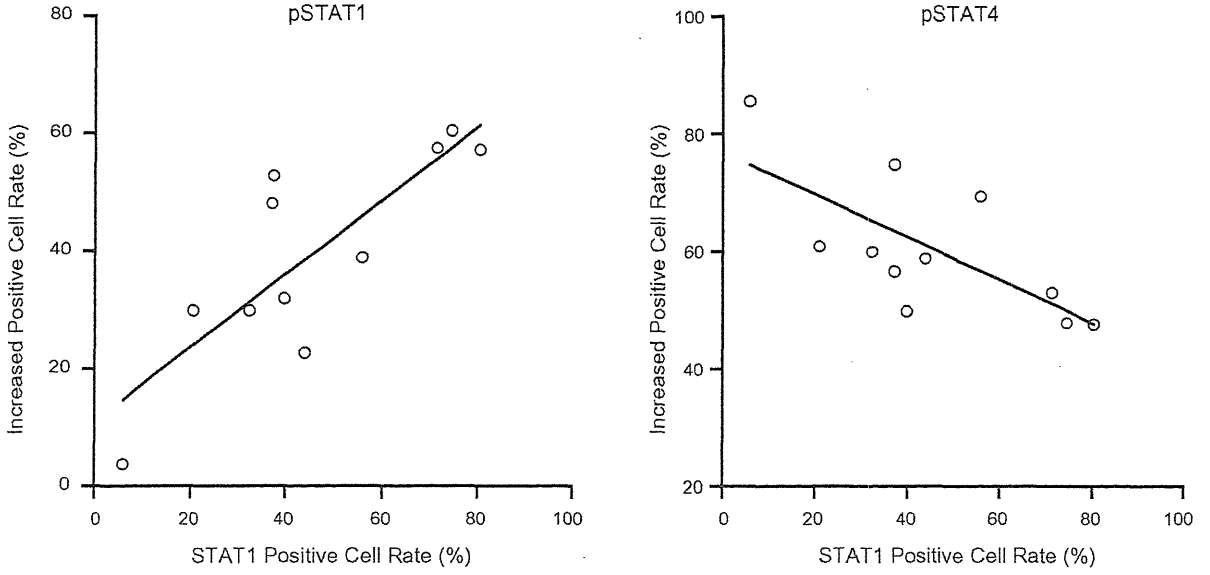

Fig. 4. Correlation between STAT1 level and pSTAT1/4 level in response to IFN-α in NK cells from patients with chronic HCV infection. The relationship was statistically analyzed between intracellular STAT1 level in NK cells and increased pSTAT1/4 level in response to IFN-α in NK cells from patients with chronic HCV infection. Each circle represents individual data. The lines represent regression lines.

which is itself a downstream gene of pSTAT1, by IFN-α based therapy, correlated negatively in vivo with the basal STAT1 expression level before therapy (Miyagi et al. unpublished data). The higher basal STAT1 expression causes a greater level of STAT1 phosphorylation in response to IFN-α, which is followed by a greater level of SOCS1 induction and then might result in a lower increase of STAT1 level. Since perforin and granzyme B are also ISGs from the pSTAT1 pathway [6,25], it is reasonable that the mRNA induction of perforin and granzyme B in response to IFN-α in NK cells from the CHC patients was not significantly greater but modestly lower than those from the HS (Fig. 5). Indeed, the enhancement of degranulation by IFN-α, that is, the increase of CD107a expression, in the presence of K562 cells in response to IFN-α, was significant in NK cells from the HS, but not in those from the CHC patients (Fig. 6).

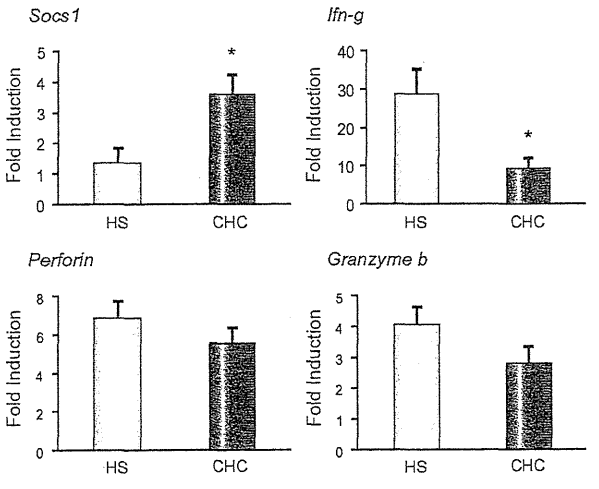

Fig. 5. Induction of ISGs in NK cells in response to IFN-α *in vitro*. NK cells were purified from PBMCs derived from patients with chronic HCV infection (CHC) and healthy subjects (HS). Isolated NK cells were untreated or treated with natural IFN-α *in vitro* for 3 h, and then collected. The collected cell RNA level of the indicated genes and β-actin as a control were analyzed by real-time RT-PCR. Data are shown as the fold increase of treated cells compared with untreated cells, with means ± standard error of the mean from five subjects in each group. *p <0.05 vs. HS.

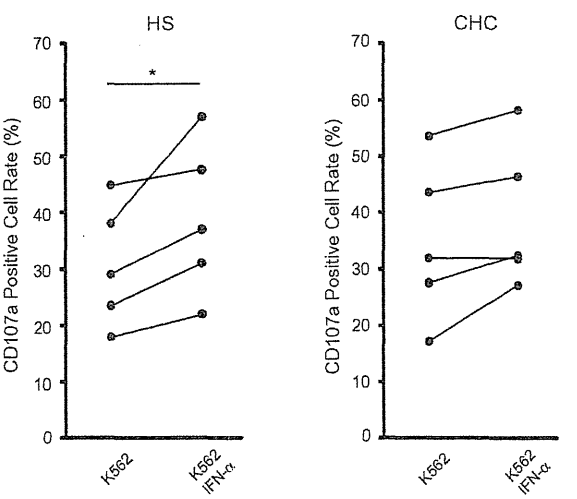

Fig. 6. Increase of NK cell degranulation by IFN-α stimulation. PBMCs derived from patients with chronic HCV infection (CHC) and healthy subjects (HS) were treated with or without IFN-α in the presence of K562 cells. The CD107a expression of NK cells were evaluated by flow cytometry, electronically gating on $CD56^+$ $CD3^-$ NK cells. Data are shown as the frequency of CD107a-positive NK cells treated with or without IFN-α. Each circle represents individual data. *p <0.05.

Patients who were clear of HCV due to IFN-α based therapy exhibited a significant increase in NK cell numbers and activity in the peripheral blood as well as in the liver compared to those who were not able to become clear of the virus [26–28]. IFN-γ produced from NK cells have been reported to suppress HCV replication in vitro [29]. IFN-γ from NK cells is also considered to activate the subsequent adaptive immune response during virus infection as well as inhibit viral replication [1,2,7]. These findings suggest the involvement of NK cells with IFN-γ in the response to IFN-α based therapy. The present study showed that the level of STAT4 phosphorylation in response to IFN-α in NK cells correlated negatively with the intracellular STAT1 level in NK cells (Fig. 4), and that IFN-γ induction, which is one of the downstream genes of pSTAT4, was clearly weaker in NK cells from the patients with CHC than in those from the HS (Fig. 5). The lower activation in CHC patients of the pSTAT4-to-IFN-γ pathway in response to IFN-α in NK cells compared to those from the HS might be one of the mechanisms which make CHC patients resistant to IFN-α based therapy.

Ahlenstiel et al. have recently reported that chronic exposure to HCV-induced IFN-α caused NK cells to become functionally polarized towards a cytotoxic phenotype, but that lacked an increase in IFN-γ production [30]. Moreover, Oliviero et al. showed that NK cells from CHC patients were of a predominantly activating phenotype, and that these phenotypic changes were associated with enhanced cytotoxic activity and defective IFN-γ production [31]. These reports would be associated with our finding that NK cells from the CHC patients displayed a high level of STAT1 expression. Cytotoxic molecules such as perforin and granzyme, as well as STAT1, belong to the ISGs [6,25]. A high level of STAT1 in NK cells in the CHC patients might correspond to a high level of cytotoxic molecules in NK cells resulting in enhanced cytotoxic activity at the basal level. Indeed, the CD107a expression at basal level in NK cells from the CHC patients seemed to be modestly higher than that in NK cells from the HS (Fig. 6), although NK cells from the CHC patients did not significantly increase the CD107a expression in response to IFN-α. On the other hand, our present study showed that STAT1 expression level in NK cells correlated negatively with the activation of STAT4 to produce IFN-γ in response to IFN-α in NK cells. A high level of STAT1 in NK cells would also cause defective IFN-γ production in the NK cells of patients with CHC.

Recent studies have revealed that the higher level of ISGs in hepatocytes as well as in PBMCs before IFN-α based therapy is associated with resistance to this therapy [32–33]. The present study demonstrated that NK cells from CHC patients displayed higher levels of STAT1, which is one of the ISGs, compared with those from HS (Fig. 2). Those who had a higher STAT1 level in NK cells showed less STAT4 phosphorylation and more STAT1 phosphorylation in response to IFN-α, resulting in less IFN-γ induction and more SOCS1 induction. Thus, it is possible that those who have a higher STAT1 level in NK cells would display less response to IFN-α based therapy. Our preliminary data with a small number of patients treated with IFN-α based therapy revealed a tendency for those who had a higher STAT1 level in NK cells to not respond well to the therapy in the context of HCV clearance by week 8 after initiation of therapy (Supplementary Fig. 3).

In the present study, we found that the expression level of total STAT1, a key molecule of IFN-α signaling, was clearly higher in NK cells from the patients with CHC than in those from the HS. The phosphorylation levels of STAT1 and STAT4 with IFN-α stimulation were altered in NK cells from the CHC patients, compared with those from the HS. The induction of IFN-γ mRNA expression with IFN-α stimulation, which is one of the downstream genes of pSTAT4, was clearly weaker in isolated NK cells from the CHC patients than in those from the HS. The induction of SOCS1 mRNA expression, which is one of the downstream genes of pSTAT1, was clearly stronger. The enhancement of NK cell degranulation, the increase of CD107a expression, in response to IFN-α was significant in the HS, but not in the CHC patients. These results indicate that IFN-α signaling in NK cells is altered in CHC patients, suggesting that this alteration of IFN-α signaling is associated with the persistence of chronic HCV infection and resistance to IFN-α therapy. The basal total STAT1 level in NK cells might enable the prediction of the outcome of IFN-α therapy against HCV infection, and thus could serve as a molecular target for more effective IFN-α based therapy.

Conflict of interests

The authors who have taken part in this study declare that they do not have anything to disclose regarding funding or conflict of interest with respect to this manuscript.

Acknowledgements

This work was supported by Grants-in-aid for Scientific Research (to T. Takehara and T. Miyagi) and Global Centers of Excellence Program (to T. Miyagi) from the Ministry of Education, Culture, Sports, Science and Technology of Japan.

Supplementary data

Supplementary data associated with this article can be found, in the online version, at doi:10.1016/j.jhep.2010.03.018.

References

[1] Biron CA, Nguyen KB, Pien GC, Cousens LP, Salazar-Mather TP. Natural killer cells in antiviral defense: function and regulation by innate cytokines. Annu Rev Immunol 1999;17:189–220.
[2] Farrar MA, Schreiber RD. The molecular cell biology of interferon-gamma and its receptor. Annu Rev Immunol 1993;11:571–611.
[3] García-Sastre A, Biron CA. Type 1 interferons and the virus–host relationship: a lesson in détente. Science 2006;312:879–882.
[4] Cho SS, Bacon CM, Sudarshan C, Rees RC, Finbloom D, Pine R, et al. Activation of STAT4 by IL-12 and IFN-alpha: evidence for the involvement of ligand-induced tyrosine and serine phosphorylation. J Immunol 1996;157:4781–4789.
[5] Matikainen S, Paananen A, Miettinen M, Kurimoto M, Timonen T, Julkunen I, et al. IFN-alpha and IL-18 synergistically enhance IFN-gamma production in human NK cells: differential regulation of Stat4 activation and IFN-gamma gene expression by IFN-alpha and IL-12. Eur J Immunol 2001;31:2236–2245.
[6] Liang S, Wei H, Sun R, Tian Z. IFNalpha regulates NK cell cytotoxicity through STAT1 pathway. Cytokine 2003;23:190–199.
[7] Lee SH, Miyagi T, Biron CA. Keeping NK cells in highly regulated antiviral warfare. Trends Immunol 2007;28:252–259.
[8] Liang TJ, Rehermann B, Seeff LB, Hoofnagle JH. Pathogenesis, natural history, treatment, and prevention of hepatitis C. Ann Intern Med 2000;132:296–305.

Research Article

[9] Kamal SM, Fouly AE, Kamel RR, Hockenjos B, Al Tawil A, Khalifa KE, et al. Peginterferon alfa-2b therapy in acute hepatitis C: impact of onset of therapy on sustained virologic response. Gastroenterology 2006;130:632–638.

[10] Manns MP, McHutchison JG, Gordon SC, Rustgi VK, Shiffman M, Reindollar R, et al. Peginterferon alfa-2b plus ribavirin compared with interferon alfa-2b plus ribavirin for initial treatment of chronic hepatitis C: a randomised trial. Lancet 2001;358:958–965.

[11] Fried MW, Shiffman ML, Reddy KR, Smith C, Marinos G, Gonçales FL, et al. Peginterferon alfa-2a plus ribavirin for chronic hepatitis C virus infection. N Engl J Med 2002;347:975–982.

[12] Santantonio T, Fasano M, Sinisi E, Guastadisegni A, Casalino C, Mazzola M, et al. Efficacy of a 24-week course of PEG-interferon alpha-2b monotherapy in patients with acute hepatitis C after failure of spontaneous clearance. J Hepatol 2005;42:329–333.

[13] Takehara T, Hayashi N. Natural killer cells in hepatitis C virus infection: from innate immunity to adaptive immunity. Clin Gastroenterol Hepatol 2005;3:S78–S81.

[14] Golden-Mason L, Rosen HR. Natural killer cells: primary target for hepatitis C virus immune evasion strategies? Liver Transpl 2006;12:363–372.

[15] Szabo G, Chang S, Dolganiuc A. Altered innate immunity in chronic hepatitis C infection: cause or effect? Hepatology 2007;46:1279–1290.

[16] Jinushi M, Takehara T, Tatsumi T, Kanto T, Miyagi T, Suzuki T, et al. Negative regulation of NK cell activities by inhibitory receptor CD94/NKG2A leads to altered NK cell-induced modulation of dendritic cell functions in chronic hepatitis C virus infection. J Immunol 2004;173:6072–6081.

[17] Takehara T, Uemura A, Tatsumi T, Suzuki T, Kimura R, Shiotani A, et al. Natural killer cell-mediated ablation of metastatic liver tumors by hydrodynamic injection of IFNalpha gene to mice. Int J Cancer 2007;120:1252–1260.

[18] Miyagi T, Gil MP, Wang X, Louten J, Chu WM, Biron CA. High basal STAT4 balanced by STAT1 induction to control type 1 interferon effects in natural killer cells. J Exp Med 2007;204:2383–2396.

[19] Alter G, Malenfant JM, Altfeld M. CD107a as a functional marker for the identification of natural killer cell activity. J Immunol Methods 2004;294:15–22.

[20] Alexander WS, Hilton DJ. The role of suppressors of cytokine signaling (SOCS) proteins in regulation of the immune response. Annu Rev Immunol 2004;22:503–529.

[21] Pfeffer LM, Madey MA, Riely CA, Fleckenstein JF. The induction of type I interferon production in hepatitis C-infected patients. J Interferon Cytokine Res 2009;29:299–306.

[22] Dolganiuc A, Norkina O, Kodys K, Catalano D, Bakis G, Marshall C, et al. Viral and host factors induce macrophage activation and loss of toll-like receptor tolerance in chronic HCV infection. Gastroenterology 2007;133:1627–1636.

[23] Der SD, Zhou A, Williams BR, Silverman RH. Identification of genes differentially regulated by interferon alpha, beta, or gamma using oligonucleotide arrays. Proc Natl Acad Sci USA 1998;95:15623–15628.

[24] Ji X, Cheung R, Cooper S, Li Q, Greenberg HB, He XS. Interferon alfa regulated gene expression in patients initiating interferon treatment for chronic hepatitis C. Hepatology 2003;37:610–621.

[25] Zimmerer JM, Lesinski GB, Kondadasula SV, Karpa VI, Lehman A, Raychaudhury A, et al. IFN-alpha-induced signal transduction, gene expression, and antitumor activity of immune effector cells are negatively regulated by suppressor of cytokine signaling proteins. J Immunol 2007;178:4832–4845.

[26] Bonavita MS, Franco A, Paroli M, Santilio I, Benvenuto R, De Petrillo G, et al. Normalization of depressed natural killer activity after interferon-alpha therapy is associated with a low frequency of relapse in patients with chronic hepatitis C. Int J Tissue React 1993;15:11–16.

[27] Appasamy R, Bryant J, Hassanein T, Van Thiel DH, Whiteside TL. Effects of therapy with interferon-alpha on peripheral blood lymphocyte subsets and NK activity in patients with chronic hepatitis C. Clin Immunol Immunopathol 1994;73:350–357.

[28] Yamagiwa S, Matsuda Y, Ichida T, Honda Y, Takamura M, Sugahara S, et al. Sustained response to interferon-alpha plus ribavirin therapy for chronic hepatitis C is closely associated with increased dynamism of intrahepatic natural killer and natural killer T cells. Hepatol Res 2008;38:664–672.

[29] Wang SH, Huang CX, Ye L, Wang X, Song L, Wang YJ, et al. Natural killer cells suppress full cycle HCV infection of human hepatocytes. J Viral Hepat 2008;15:855–864.

[30] Ahlenstiel G, Titerence RH, Koh C, Edlich B, Feld JJ, Rotman Y, et al. Natural killer cells are polarized toward cytotoxicity in chronic hepatitis C in an interferon-alfa-dependent manner. Gastroenterology 2010;138:325–335.

[31] Oliviero B, Varchetta S, Paudice E, Michelone G, Zaramella M, Mavilio D, et al. Natural killer cell functional dichotomy in chronic hepatitis B and chronic hepatitis C virus infections. Gastroenterology 2009;137:1151–1160.

[32] Feld JJ, Nanda S, Huang Y, Chen W, Cam M, Pusek SN, et al. Hepatic gene expression during treatment with peginterferon and ribavirin: identifying molecular pathways for treatment response. Hepatology 2007;46:1548–1563.

[33] Sarasin-Filipowicz M, Oakeley EJ, Duong FH, Christen V, Terracciano L, Filipowicz W, et al. Interferon signaling and treatment outcome in chronic hepatitis C. Proc Natl Acad Sci USA 2008;105:7034–7039.